Multivariable process control in high temperature and high pressure environment using non-intrusive multi sensor data fusion

Olav Gerhard Haukenes Nygaard
Telemark University College
Faculty of Technology
Porsgrunn, Norway

Thesis submitted to the
Norwegian University of Science and Technology
for the degree of doktor ingeniør (dr.ing.)

Doctoral thesis at NTNU 2006:38

ISBN 82-471-7819-2 (electronic issue)
ISBN 82-471-7820-6 (printed issue)

September, 2006

Preface

This thesis is submitted as a part of the requirements for the academic degree of *doktor ingeniør* at the Norwegian University of Science and Technology (NTNU) and Telemark University College (HiT). The research has been carried out as a part of the MULTIPROCON research program which is funded by the Research Council of Norway and Telemark Technological Research & Development Centre (Tel-Tek). The International Research Institute of Stavanger (IRIS) has also been supporting this work by providing offices and valuable guidance during my research period.

First I would like to thank my advisor, Professor Dr. Saba Mylvaganam at Department of Electrical Engineering, Information Technology and Cybernetics for encouraging me prior to and during my PhD project. His ideas and visions for using multi sensor data fusion in process control have been a great motivation.

I am in great debt to my co-advisor, Professor Dr. Erlend H. Vefring, who is Vice President - Petroleum at IRIS Petroleum. He has guided me and encouraged me all the way during my PhD-project. Thanks also to my other co-advisor, Professor Dr. Morten Chr. Melaaen at Department of Process, Energy and Environmental Technology, for supporting me in the difficult periods. And in the memory of the late Jørn Archer, former Head of Department of Electrical Engineering, Information Technology and Cybernetics: Thanks Jørn, for your enthusiasm and supporting advice.

Special thanks also to Chief Scientist Dr. Geir Nævdal, Dr. Kjell-Kåre Fjelde, Dr. Ove Sævareid, and Dr. Rolf Johan Lorentzen, for all the fruitful discussions and your patience while I learned more and more from you all. Thanks also to Dr. Erling Aarsand Johannessen for giving me useful comments while finalizing the thesis. Thanks also to my other colleagues at IRIS Petroleum.

Thanks to my other colleagues at Telemark University College, especially to Urmila Datta, Dr. Geir Werner Nilsen, Kjetil Fjalestad, Dr. Tor Anders Hauge, Dr. Glenn-Ole Kaasa, Dr. Martha Dueñas Díez, Beathe Furenes, Nils-Olav Skeie and Kjell Joar Alme. Also thanks to the staff members:

Professor Dr. Bernt Lie, Professor Dr. Rolf Ergon, Rolf Palmgren, Morten Pedersen, Talleiv Skredtveit and Eivind Fjelddalen.

Thanks to my dear parents, Jofrid and Nils, for a lifetime of unlimited love and support. Thanks to my dear parents-in-law, Inger and Nils, for loving support during all these years. At last, thousands of thanks to the woman in my life, my dearest wife Cathrine, you are the very best, and thanks to our lovely children Nikolai, Mattias, Sofie and Emilie, for all your love and care.

Summary

The main objective of this thesis is to use available knowledge about a process and combine this with measurement data from the same process to extract more information about the process. The combination of knowledge and measurement data is referred to as Multi Sensor Data Fusion, MSDF. This added information is then used to control the process towards a specified goal.

The process studied in this thesis is the process of drilling wells in a petroleum reservoir, while the oil is flowing from the reservoir. In the petroleum industry, this is defined as underbalanced drilling (UBD), where the bottom hole pressure (BHP) in the well is below the pore pressure in the reservoir.

Detailed knowledge of the process is of paramount importance when using multi sensor data fusion. Due to this, various process modelling efforts are examined and evaluated, from simple relations between parameters to a finite-element approach of modelling the fluid flow in the well during drilling.

Several sensors are used in the various cases, and existing sensors such as pressure sensors and flow sensors are the main data source in the analysis. Future scenario with sensors such as pressure arrays and non-intrusive multiphase flow meters are evaluated. In addition, new positions of existing sensor systems are discussed.

The methods available for fusing the knowledge of the process represented as models together with the available data is ranging from artificial intelligent methods such as neural networks, to methods incorporating statistical analysis such as various Kalman filters. History matching techniques using gradient techniques are also examined.

The migration of reservoir fluids into the well during UBD influences the BHP of the well. The results in the thesis show that this reservoir influx can be calculated by estimating some of the important reservoir parameters such as reservoir pore pressure or reservoir permeability. These reservoir parameters can be estimated most efficiently by performing an MSDF using a detailed nonlinear model of the well and reservoir dynamic behaviour to-

gether with real-time measurements of the fluid flow parameters such as fluid temperature, fluid pressure and fluid flow rates. The unscented Kalman filter shows the best performance when evaluating both estimation accuracy and computational requirements.

Regarding available instrumentation for use during UBD, the analysis shows that there is a major potential in introducing new sensors. As new data transmission methods are emerging and making data from sensors distributed along the drillstring available, this can generate a shift in paradigm regarding real-time analysis of reservoir properties during drilling.

Controlling the process is an important usage of the information gained from the MSDF analysis. Various control methods for controlling the most important process variables are examined and evaluated. The results show that acceptable pressure control can be obtained when using the choke valve opening as the primary control parameter. However, the choke valve operation has to be closely coordinated with drilling fluid flow rate adjustments. The choke valve opening control is able to compensate for pressure variations during the whole drilling operation.

A suggested nonlinear model predictive control algorithm gives best results when looking at the control accuracy, and can easily be expanded to handle multiple control inputs and system constraints. This control algorithm uses a detailed model of the well and reservoir dynamics. The Levenberg-Marquardt algorithm is used to calculate the optimal future control variables. The main drawback of the control algorithm is computational burden. A linear control algorithm, which also is evaluated, uses less computational resources, but has less control accuracy and is more difficult to expand into a multivariable control system.

Recommendations for further work are to expand the suggested model predictive control algorithm to handle more control inputs, while reducing the computational burden by incorporating low-order models for describing the future behaviour of the well.

Contents

Nomenclature

List of symbols

a	Output value of single artificial neuron
$\mathbf{a}$	Acceleration
A_a	Cross sectional area of annulus
A_d	Cross sectional area of drillstring
$\mathbf{A}^i$	Hessian matrix at optimization search step i
b	Bias of neural network input value
$B(\cdot)$	Function for calculating gene binary representation from parameter value
$B^{-1}(\cdot)$	Inverse function for calculating parameter value from gene binary representation
c	Reservoir fluid compressibility
c_p	Specific heat capacity
C	Valve discharge coefficient
D	Equivalent hydraulic diameter of pipe
$\mathbf{D}^i$	Diagonal matrix at optimization search step i
e	Error between reference parameter and measured parameter
$f(\cdot)$	Neuron transfer function
$f[\cdot]$	State function
$f_p[\cdot]$	State function for predictions
f_{mix}	Friction factor of mixture
$\mathbf{F}$	Force
$\mathbf{F}_k$	Linearized function of $f[\cdot]$ at time step k
g	Acceleration due to gravity
h	True vertical depth of well
h	Height of reservoir section interface with well
$h[\cdot]$	Measurement function
$h_p[\cdot]$	Measurement function for predictions
H_p	Prediction horizon
$\mathbf{H}_k$	Linearized function of $h[\cdot]$ at time step k
$\mathbf{J}^i$	Jacobian matrix at optimization search step i

k	Sensor indexing value
k	Time indexing value
K	Reservoir permeability
K_f	Feed-forward control gain
K_p	Feed-back proportional control gain
$\mathbf{K}_k$	Kalman gain at time step k
L	Length of well
L_0	Initial well length
m	Mass
m_a	Mass in annulus
m_d	Mass in drillstring
m_g	Mass of gas
m_l	Mass of liquid
n	Input value for neuron transfer function
n	Number of measurements
$\mathbf{N}(\cdot)$	Normal probability distribution
p	Pressure
p_a	Annulus pressure
p_{atm}	Atmospheric pressure
p_{bit}	Pressure at bit
p_{coll}	Reservoir collapse pressure
p_c	Compression pressure
p_{choke}	Pressure at choke valve
p_d	Drillstring pressure
p_f	Friction pressure loss
p_{frac}	Reservoir fracture pressure
p_h	Hydrostatic pressure
p_{pump}	Pump pressure
p_{res}	Reservoir pore pressure
p_{well}	Annulus pressure
$\mathbf{p}$	Neural network layer input vector
P	Set of NMPC coincidence points
$\mathbf{P}_k^a$	Analysed estimation error covariation matrix at timestep k
$\mathbf{P}_k^f$	Forecasted estimation error covariation matrix at timestep k
q_i	Injected fluid volume flow rate
q_o	Original fluid volume flow rate
q_w	Reservoir fluid volume flow rate into well
Q	Thermodynamic energy
$\mathbf{Q}_k$	Model error covariation matrix at time step k
r	Control reference value

$\mathbf{r}_k(\cdot)$	Difference between measured and modelled sensor value at time step k
$\mathbf{r}^i(\cdot)$	Difference between measured and modelled sensor value at optimization search step i
$\mathbf{r}^j(\cdot)$	Difference between measured and modelled sensor value j
r_w	Well radius
R_{mf}	Drilling mud resistivity
R_t	Deep resistivity
R_{xo}	Shallow resistivity
R_w	SP-log resistivity
Re_{mix}	Reynolds number for mixture
$\mathbf{R}_k$	Measurement noise covariation matrix at time step k
S	Well-reservoir interface skin factor
$S(\cdot)$	Minimization objective function
S_w	Reservoir water saturation
t	Time
T_r	Temperature of fluid mixture after mixing
T_o	Original fluid temperature before mixing
T_i	Injected fluid temperature before mixing
T_i	Integral time for PI-controller
u	Control variable
u_{max}	Maximum control variable
u_{min}	Minimum control variable
v	Process disturbance
v_d	Vertical drilling rate
v_g	Gas velocity
v_l	Liquid velocity
v_{mix}	Well fluid velocity
$\mathbf{v}_0$	Initial model error standard deviation at time step 0
$\mathbf{v}_k$	Model error standard deviation at time step k
w_{bit}	Fluid mass rate at bit
w_{choke}	Fluid mass rate at choke
w_g	Gas mass rate
w_{in}	Mass rate into well
w_l	Liquid mass rate
w_{pump}	Fluid mass rate at pump
w_{mix}	Fluid mixture mass rate
w_{res}	Fluid mass rate from reservoir
w	Valve mass flow rate
w_{out}	Mass rate out of well
$\mathbf{w}_k$	Measurement noise standard deviation at time step k

$\mathbf{w}_k^{(j)}$	Measurement noise standard deviation at time step k for ensemble member j
W_c	UKF weight matrix for covariance calculation
W_m	UKF weight matrix for mean calculation
$\mathbf{W}$	Neural network weight matrix
$\mathbf{x}_k$	State vector at time step k
y	Measured value
y_{max}	Upper bound of measured value
y_{min}	Lower bound of measured value
y_{ref}	Reference pressure
y_k^c	Calculated value of sensor k
y_k^m	Measured value of sensor at time step k
y_k^m	Measured value of sensor k
$\mathbf{y}_k$	Measurement vector at time step k
$\mathbf{y}_k^{m(j)}$	Measurement vector at time step k for ensemble member j
z	Well length
z	Valve opening area
α	UKF filter sigma point design parameter
α_g	Gas void fraction
α_l	Liquid void fraction
β	UKF filter sigma point design parameter
γ	Eulers constant = 0.5772
δ^i	Optimization search step for parameter vector
Δp	Differential pressure across valve
ΔT	Differential temperature
ϵ/d	Relative roughness of pipe
θ	Well angle from vertical
θ	Model parameters
θ_b	Binary representation of model parameters
θ^i	Model parameters at optimization search step i
θ_{min}	Minimum value for model parameters
θ_{max}	Maximum value for model parameters
λ^i	Levenberg-Marquardt Constant
λ	UKF design parameter
μ	mean in a normal probability distribution
μ	Fluid viscosity
μ_{mix}	Fluid mixture viscosity
π	$= 3.141592\ldots$
σ	standard deviation in a normal probability distribution
ρ_g	Gas density
ρ_l	Liquid density

ρ_{mix}	Fluid mixture density
ϕ	Reservoir porosity
χ	Augmented state vector
χ_k^a	Analysed augmented state vector at time step k
$\chi_k^{a(j)}$	Analysed augmented state vector of ensemble member j at time step k
χ_k^f	Forecasted augmented state vector at time step k
$\chi_k^{f(j)}$	Forecasted augmented state vector of ensemble member j at time step k
χ_k^t	True augmented state vector at time step k
χ_k^σ	UKF sigma augmented state vector at time step k

List of abbreviation

API	American Petroleum Institute
BHP	Bottomhole Pressure
EKF	Extended Kalman Filter
EnKF	Ensemble Kalman Filter
JDL	United States Joint Director's of Laboratories
LM	Levenberg-Marquardt
LWD	Logging While Drilling
MPC	Model Predictive Control
MSDF	Multi Sensor Data Fusion
MWD	Measurement While Drilling
NI	National Instruments
NMPC	Nonlinear Model Predictive Control
NMR	Nuclear Magnetic Resonance
PI	Production Index (reservoir)
PI	Proportional Integral (control parameters)
SP	Spontaneous Potential
TVD	True Vertical Depth
UBD	UnderBalanced Drilling
UKF	Unscented Kalman Filter

Part I

Introduction

Chapter 1

Background

During the drilling of wells in petroleum reservoirs, a drilling fluid is used to transport the cuttings and particles from the drilling process at the drill bit to the surface. The pressure in the well during drilling is a function of the hydrostatic and dynamic pressure in the well. During conventional drilling, the well pressure is kept higher than the reservoir pressure using the drilling fluid density as the main adjustable parameter. This pressure overbalance is due to safety considerations, since the main reason for having higher pressure in the well than the reservoir is to avoid situations where the reservoir fluid is flowing uncontrolled into the well and further up to the surface. Conventional drilling has some drawbacks since the pressure overbalance causes the drilling fluid which contains particles to penetrate into the porous sections of the formation. These particles obstruct the flow from the reservoir when the well is set into production.

To enhance the production from a petroleum reservoir, new drilling techniques have been developed during the last decade. A drilling technique that has shown to give better drainage of the reservoir during production, is the method of underbalanced drilling (UBD) [48]. During UBD the well pressure is kept below the reservoir pore pressure. Knowledge of the pore pressure in the reservoir formation can be gathered from the well tests performed during the exploration drilling.

However, the reservoir formation has variations in the pore pressure that is difficult to estimate prior and during the drilling operation. This is especially difficult if the reservoir consists of several different layers including formation faults. In addition, the bottomhole well pressure is difficult to keep within defined margins. The well pressure is influenced by several factors such as variations in the drilling fluid properties. Also, the fluid viscosity and the flow rate cause a pressure loss along the well. There is a possibility of measuring the pressure, but a low data transfer rate between the drill

bit and the surface makes it difficult to obtain information about pressure transients.

There is a need for improving the methods for estimating the reservoir pore pressure during drilling. In addition, the various factors that influence the well pressure during drilling operations should be further understood and analysed. Methods for automating the control of the pressure balance between the pore pressure and the well pressure should be developed and evaluated.

Chapter 2

Scope of Thesis

The scope of this thesis is to develop and evaluate methods for performing multivariable process control in high temperature and high pressure environment using non-intrusive multi sensor data fusion (MSDF). MSDF is the process to combine available data regarding a system to estimate unknown properties of the system.

In UBD, there is a need for controlling the pressure balance between the reservoir pore pressure and the well pressure. This pressure balance is influenced by several variables such as the drilling fluid density, drilling fluid pump rate and well choke opening area. The high temperature and high pressure environment in the well gives severe restrictions on the use of sensors and signal transmission technologies. Direct measurements of important reservoir parameters such as reservoir pressure are not available, and estimation of these parameters has to be performed by combining data from several sensors, including non-intrusive sensors. The use of MSDF is required to evaluate the sensor data originating from several different sources, including time and space variations. MSDF makes it possible to extract more information from the sensors compared to the information gathered when looking at each sensor individually.

In this thesis, MSDF methods for estimating both pore pressure and well pressure during drilling operations are presented. Several sensor systems are evaluated, and suggestions for future non-intrusive sensor designs have been included. Investigations on implementing non-intrusive sensors have also been discussed. The main focus has been to fuse flow related data typically available from the drilling system. This flow related data includes flow rate, flow composition, pressures and temperature at various positions of the drilling system.

In addition, different control methods are developed and tested in various cases where the focus is to maintain the UBD conditions during the whole

drilling operation.

The bottomhole pressure and the reservoir pore pressure are difficult both to measure and to estimate. Other data about the system must be included to extract additional information about the drilling process. The data from various sensors and sources are combined both in time and space such that more detailed information about the whole process is revealed. Several methods for making use of the data are used in this thesis, such as dynamic modelling and least-squares parameter estimation methods.

Having developed methods for estimating the pore pressure and the bottomhole well pressure, various methods for controlling the well pressures according to the reference values are described and evaluated. Multiple control inputs can be used, such as drilling fluid flow rate, drilling fluid density[1] and also choke valve opening area. Simple control methods based on previous experience and linear control laws are examined, as well as more advanced non-linear model predictive control methods. By combining the parameter estimation methods and the control methods, underbalanced conditions can be achieved in the well during the whole drilling operation.

The thesis is divided into two main parts. Part I is divided into nine chapters. Chapter 1 gives some background information regarding petroleum well drilling and discusses the current challenges. Chapter 2 presents the scope of the thesis and the thesis contributions. Chapter 3 focuses on the process of UBD in more detail. Chapter 4 presents MSDF, with details on sensors, models, and fusion methods, and in Chapter 5 examples of using MSDF are given. Chapter 6 presents the process control methods used for controlling the well pressure during UBD. In Chapter 7, a short description of the research project progression and a presentation of the papers included in the thesis are given. Chapter 8 discusses possible future research directions, and Chapter 9 presents the conclusions of the thesis.

In Part II, five papers published in conjunction with this thesis are given.

In Paper A, *Reservoir Characterization during Underbalanced Drilling: Methodology, Accuracy, and Necessary Data* an existing two-phase well fluid flow model is expanded to include fluid flow from the reservoir. The reservoir permeability or reservoir pressure is estimated by minimizing the difference between the model states and the synthetically generated measurement data, using a post-drilling analysis solving a least-squares problem using the Levenberg-Marquardt algorithm.

In Paper B, *Reservoir Characterization during Underbalanced Drilling (UBD): Methodology and Active Tests*, perturbations of the well pressure

[1]The fluid density can be adjusted by changing the fluid mixing ratio of two drilling fluids where one fluid has higher density than the other [88].

were applied to examine if this made the parameter estimation introduced in Paper A easier. The results show that the reservoir pore pressure and the reservoir permeability are simultaneously estimated based on synthetically generated measurement data. In addition to parameter estimation where the Levenberg-Marquardt algorithm is used in solving a least squares problem, the ensemble Kalman filter algorithm has also been examined, enabling the possibility of performing parameter estimation during the actual drilling operation.

In Paper C, *Underbalanced Drilling: Improving Pipe Connection Procedures Using Automatic Control*, the performance of the unscented Kalman filter algorithm is examined, estimating the reservoir permeability. The analysis is performed using synthetically generated measurement data. In addition, a model predictive control algorithm is presented and used to maintain correct well pressure during a pipe connection procedure.

In Paper D, *Bottomhole Pressure Control During Pipe Connection in Gas Dominant Wells*, the validity of the two-phase flow model is examined by comparing model data with measurement data from a full-scale test well facility. In addition, the model predictive control algorithm including the unscented Kalman filter parameter estimation algorithm is evaluated when simulating a drilling scenario in a multi-layer reservoir having a complex two-phase flow regime in the well. The control system simulations perform well applied to synthetically generated measurement data.

In Paper E, *Non-linear model predictive control scheme for stabilizing annulus pressure during oil well drilling*, the model predictive control algorithm is compared with a linear control algorithm. A low-order state model is developed and compared with the existing detailed model. The low-order state model is used for defining the linear control parameters. The linear control algorithm is compared with both manual control and the model predictive control algorithm. The results show that the linear control algorithm gives less fluctuations compared with manual control. When comparing the results using the linear control algorithm and the model predictive control algorithm, the model predictive control algorithm gives the least fluctuations. This indicates that the model predictive control algorithm is superior to the linear control algorithm when focusing on accuracy performance.

The published works in this thesis are done in collaboration with other researchers, where I have written the major parts of the papers. The main contributions of this thesis are:

Modelling

- Development and implementation of a dynamic reservoir model for use together with a dynamic, multiphase flow model.
- Updating the detailed dynamic flow model to allow for active choke control.
- Development and implementation of a low-order state model for two phase fluid flow designed for UBD operations.

Sensors

- Evaluation of various types of sensor arrays based on pressure and temperature measurements for estimation of inflow in UBD operations.
- Evaluation of the use of downhole flow sensors during underbalanced operations.

Data Fusion

- Comparison of a neural net classification method and a history matching method for estimating pipe inflow in a laboratory test rig.
- Comparison of history matching methods versus the ensemble Kalman filter for estimation of multiple reservoir parameters using fluid flow measurements and detailed fluid flow model of well-reservoir interaction.
- Describing and evaluating a methodology for real-time reservoir characterization during UBD operations using the unscented Kalman filter.

Process Control

- Design, implementation and evaluation of an MPC algorithm using a non-linear optimization algorithm and a detailed well-reservoir model.

The implementation of the detailed dynamic multiphase flow model was performed by other researches. The Levenberg-Marquardt optimization algorithm and the Kalman filters were implemented by other researches.

Chapter 3

Underbalanced Drilling

When drilling into a formation, the pressure in the well is critical for the success of the drilling process. The pressure in the well p_{well} must be within the operating pressure range of the formation. The upper bound of the pressure range is the formation fracturing pressure p_{frac}, the lower bound is the formation collapse pressure p_{coll}, that is

$$p_{coll}(t,x) < p_{well}(t,x) < p_{frac}(t,x), \tag{3.1}$$

where x is the position along the well trajectory and t is the time.

When drilling into a reservoir formation, the difference between the reservoir pore pressure and the well pressure represent the primary safety barrier for avoiding uncontrolled influx of reservoir fluids into the well, such as a blow-out situation. During conventional drilling, the well pressure is maintained above the reservoir pore pressure, referred to as overbalanced drilling. UBD is defined as having the well pressure below the reservoir pore pressure p_{res} during the whole drilling operation, i.e.

$$p_{coll}(t,x) < p_{well}(t,x) < p_{res}(t,x) < p_{frac}(t,x). \tag{3.2}$$

where the reservoir pore pressure p_{res} is a function of both time and position along the well trajectory. All these pressures are unknown before drilling the well.

UBD reduces the skin damage, which is caused by penetration of drilling fluids and cuttings into the reservoir. The drilling fluids that penetrate into the reservoir near the well, is referred to as "mud cake". This mud cake results in poor drainage of the reservoir when the well is set into production after the well has been completed. The removal of cuttings (hole cleaning) is also better, and this leads again to faster drill rate. However, the drawback of UBD is that the primary pressure barrier against a blow-out situation has to be replaced by some other system than the drilling fluid density.

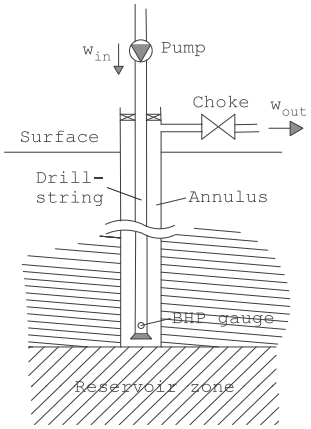

Figure 3.1: Schematic layout of an oil well drilling system prior to drilling into the reservoir.

During drilling, a drilling fluid is circulated through the drillstring and drill bit. The drill bit is equipped with a check valve, which prevents the drilling fluid in the annulus to return into the drillstring. The drilling fluid flows through the annulus between the drillstring and the walls of the well. The hydrostatic pressure in the well depends on the fluid density. The hydrostatic pressure in the well p_h can be modelled as

$$p_h = \rho_{mix} g h, \tag{3.3}$$

where ρ_{mix} is the density of the fluid mixture in the annulus, g is the gravity and h is the true vertical depth (TVD) of the well. In Fig. 3.1 an example of a well system is shown. The drilling fluid pump circulates the drilling fluid at the specified mass rate w_{in} and exits through the choke valve with the mass rate w_{out}. The pressure is measured at the bottom hole pressure (BHP) gauge. The fluid mixture in the annulus consists of several components. Primarily, it consists of the drilling fluid that was injected into the drillstring. In addition there will be cuttings from the drilling process that are transported away along with the drilling fluid. Also, if the well pressure is lower than the pore pressure in the reservoir section of the well, then the reservoir fluids will migrate into the well annulus.

The fluid friction inside the drillstring and the annulus influence the resulting pressure. The friction pressure loss, p_f , in a pipe can be modelled by

$$p_f = \frac{2\rho_{mix} f_{mix} L v_{mix}^2}{D}, \tag{3.4}$$

where f_{mix} is the friction factor which is related to the Reynolds number of

the mixture, L the total length of the well, D is the hydraulic diameter and v_{mix} is the mixture fluid velocity.

It is a challenge to control the well pressure gradient at all times during the drilling operation, since the pressure loss caused by fluid friction might have a dominant effect. The drillstring consists of several segments of pipe joined together, and the fluid flow must be stopped at distinct time intervals to be able to connect the pipe segments together, as the drillstring is penetrating deeper into the formation. The fluid flow fluctuation causes variations in the well pressure. Other operations during drilling, such as inserting the drillstring into the well and pulling the drillstring out of the well, also cause pressure variations in the well annulus.

One special concern while drilling a well in underbalanced conditions is when the drilling fluid density has to be lower than what is typical for drilling fluids consisting of liquid only. In such cases, gas is injected into the drillstring. The low density of the gas reduces the hydrostatic pressure, but results in additional complexity of the well fluid behaviour as it introduces two-phase fluid flow in the well. The gas will be compressed along the well trajectory, depending on the friction pressure and hydrostatic pressure.

When drilling in the reservoir zone, the pore pressure and other reservoir parameters might vary. Such parameter variations lead to changes in influx of reservoir fluids into the well annulus, which causes changes in the pressures in the well annulus.

3.1 Pressure management

The operator typically manipulates the pressures in the well manually by adjusting the pump rates and the choke valve. Also, the composition of the drilling fluid can be adjusted, by adding different fluid components such as various weight materials and other additives. These three methods for manipulation of the well pressures can be listed as the main control variables for a pressure control system:

- Fluid composition
- Fluid flow rate
- Choke valve position

Since all of these three control variables influence the BHP, the operator typically keeps the fluid composition and fluid flow rate constant, and uses the choke valve position to control the well pressure. In some cases, it is not sufficient to manipulate the choke valve during the drilling operation. One

possible problem is choke plugging, which is caused by particles from the drilling process that temporarily plugs the choke valve, due to small choke valve opening. A more automatic control system where all three control variables are used for active multivariable control is likely to improve the management of the well pressures.

This section describes how these three control variables, the fluid composition, the fluid flow rate and the choke valve position, influence the well pressure in different ways.

3.1.1 Drilling fluid composition

The composition of the drilling fluid is carefully chosen to achieve the correct properties needed for a successful drilling operation. The density of the drilling fluid is the most important property for obtaining the required pressure in the well. The drilling fluid density is adjusted by changing the composition of the drilling fluid, such as the amount of weight material (baryte) in the mixture. In addition, the density in the annulus part of the well is also influenced by particles from the drilling process and reservoir fluids that migrate into the well. When gas is injected into the well, the mixture flow becomes two-phase. Two-phase fluid flow has a rather complex behaviour including varying compressibility of the mixture.

The viscosity of the drilling fluid can also be adjusted by adding special components to the drilling fluid. Since one of the purposes of the drilling fluid is to transport the cuttings and particles from the well, the viscosity has to be within certain limits. Gelling effects of the drilling fluid have to be taken into account, especially during circulation start-up. Since the drilling fluid is generally strongly non-Newtonian, it does not have a well-defined viscosity. The viscosity also influence the Reynolds number of the mixture Re_{mix}, given by, [91]

$$Re_{mix} = \frac{\rho_{mix} v_{mix} D}{\mu_{mix}}, \tag{3.5}$$

where μ_{mix} is the viscosity of the fluid. The Reynolds number again affects the mixture friction factor f_{mix} which in laminar flow can be represented by, [91]

$$f_{mix} = \frac{64}{Re_{mix}}, \tag{3.6}$$

and in turbulent flow it can be modelled by the implicit Colebrook equation, defined by, [91]

$$\frac{1}{\sqrt{f_{mix}}} = -2.0 \log \left(\frac{\epsilon/d}{3.7} + \frac{2.51}{Re_{mix}\sqrt{f_{mix}}} \right), \tag{3.7}$$

where ϵ/d is the relative roughness of the pipe.

Viscosity affects the friction pressure loss in the well, indicating that viscosity can be a parameter for managing the pressure. However, viscosity does not have useful influence when the fluid flow is turbulent. The viscosity of the drilling fluid depends on the fluid temperature [91]. Systems for adjusting the drilling fluid temperature could be considered in some applications. If some of the fluid parameters are modified, then the new drilling fluid will have to displace the original drilling fluid before the parameter changes are fully effective. This requires that the fluid flow rate or choke valve opening is used to compensate for transient effects during fluid displacement.

3.1.2 Drilling fluid flow rate

The velocity of the drilling fluid in the annulus and the drillstring affects the friction pressure loss, resulting in a change in annulus or drillstring pressure. When the drilling fluid is mixed with gas, the drilling fluid becomes compressible, and the fluid flow velocity can be different in various positions in the well.

The fluid flow rate is typically adjusted using the pump at the drillstring, but other pump system can be used. One suggested design is the dual gradient method, where the annulus section of the well is split into an upper and a lower compartment. A pump system is then used to pump the annulus fluid to the top. A typical application for offshore wells, is to split the annulus at the seabed [72].

Another method to manipulate the pressure locally is to increase the annulus pressure by placing a pump in front of the choke valve. Adding this kind of additional complexity might require the use of automatic control methods [67, 84].

Special systems for maintaining the fluid flow during pipe connection has been developed [31]. This reduces the transient effects due to starting and stopping of the fluid circulation during such operations. However, such systems are quite complex.

3.1.3 Choke valve

The flow through a choke valve may be modelled by a simple valve equation, [51]

$$w_{mix} = Cz\sqrt{\rho_{mix}\Delta p}, \tag{3.8}$$

where w_{mix} is the mass flow rate, C is the discharge coefficient of the valve, z is the area of the valve opening, and Δp is the differential pressure across

the valve. Eq. (3.8) can be re-arranged to

$$\Delta p = \frac{1}{\rho_{mix}} \left(\frac{w_{mix}}{Cz} \right)^2. \tag{3.9}$$

By varying the valve opening, the pressure in the well can be managed.

3.2 Pressure Disturbances

During UBD there are several situations causing disturbances of the annulus pressure. This section describes some of the most important causes to pressure fluctuations, and discusses some of the efforts that can be made to reduce such fluctuations.

3.2.1 Reservoir fluid inflow

During UBD, there will be influx from the reservoir. A simple relation that may be used to model the influx, is the Production Index, referred to as PI. This is used to model the relation between the fluid flow and differential pressure between the well pressure and the reservoir pressure. The influx is calculated using the relation, [11]

$$q_{res} = PI \left(p_{res} - p_{well} \right), \tag{3.10}$$

where p_{well} is the well pressure, p_{res} is the initial pressure, q_{res} is the volume flow rate from the reservoir.

The parameter PI assumes semi-steady state conditions of a reservoir. However, during drilling, the interaction between the well and the reservoir is transient. Therefore, to model the influx during drilling, the analytical solution of the constant terminal rate formulation may be used, [11]

$$q_{res} = \frac{4\pi Kh \left(p_{res} - p_{well} \right)}{\mu \left(2S + \ln \left(\frac{4Kt}{e^{\gamma} \phi \mu c r_w^2} \right) \right)}, \tag{3.11}$$

where K is the permeability of the reservoir, S is the skin factor, h is the height of the well section that has contact with the reservoir, t is the time since the reservoir section were influenced by the well pressure, ϕ is the porosity of the reservoir, μ is the viscosity, c is the compressibility of the reservoir fluid and r_w is the well radius.

When drilling into a reservoir, some of the parameters in the formation are known from geophysical surveys and from the exploration drilling phase. Information such as the layer orientation and porosity of the formation might

be known from seismic data. Other information like the local variations of permeability and pore pressure are typically unknown. Since inflow of reservoir fluids influence the pressure gradient of the well, these parameters should be estimated during drilling.

3.2.2 Pipe connection procedure

In drilling operations, two different types of drilling equipment referred to as coiled tubing and jointed pipe, are used. When using coiled tubing, the hydraulic drilling motor is mounted at the end of a long tubing. The tubing is coiled on a large drum unit. The diameter of the coiled tubing is typically 0.1 m or less. When using coiled tubing, signal cables can be placed inside the tubing, giving continuous data to the top. However, since the diameter is small, buckling of the drillstring can occur.

The other type of drillstring is the jointed pipe. The drillstring consists of pipe segments of about 30 m that are jointed together. The diameter of the pipe is larger than the coiled tubing, typically about 0.25 m. The whole drillstring is rotating when drilling. Jointed pipe is the most used type of drilling equipment.

One drawback of the jointed pipe is that the drilling operation has to be interrupted when a new pipe segment is added to the drillstring. The circulation of the drilling fluid also has to be stopped, which causes variations in the BHP. These variations are due to the loss of friction pressure as the circulation stops. Fig. 3.2 shows the four operational steps required when the pipe connection is performed. During the first step the rotation of the drillstring is stopped, and the pumps circulating the drilling fluid is stopped. At step two, the pump is disconnected from the drillstring. At step three a new pipe segment is added to the drillstring, and at the last step the pump is reconnected, and the pumps starts to circulate drilling fluid. Then the rotation of the drillstring is re-started.

Another drawback of jointed pipe is the challenge to transport information from the downhole sensors up through the drillstring. Today, typically a mud pulse telemetry system is used to send information from the drill bit to the surface. However, during pipe connections, the mud pulse telemetry system is not in operation. Other systems might be used, such as a system sending electromagnetic signals through the formation. A new type of drillstring is emerging, which integrates a signal cable into a drillstring. This gives new possibilities for transferring signals from the bottom during drilling, but the signal cable is disconnected during pipe connections [30, 66].

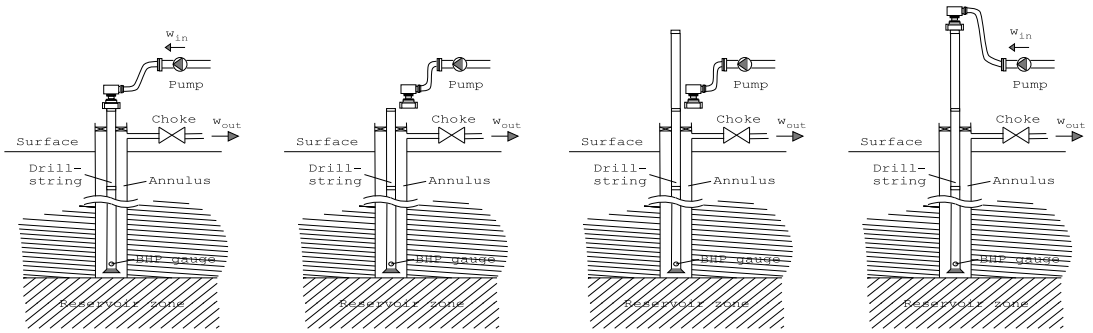

Figure 3.2: The four operational steps performed during the pipe connection procedure.

3.2.3 Other well operations

In addition to the pipe connection procedure, there are other operations causing pressure fluctuations during drilling. Rotation of the drillstring changes the flow pattern between the drillstring and the fluid in the annulus. The cuttings from the drilling process are transported along the annulus flow, and cause changes in the annulus fluid density. An increased density gives increase in the hydrostatic pressure in the annulus.

The drill bit and instrumentation at the end of the drillstring must occasionally be maintained. While the drillstring is moved, the velocity between the annulus fluid and the drillstring is changed. This velocity change leads also to pressure fluctuations [29].

Chapter 4

Multi Sensor Data Fusion in Drilling Applications

Multi Sensor Data Fusion (MSDF) is a term for using various kinds of data sources to extract more information about a process or a system. Non-intrusive sensors can also be included in the data fusion algorithms. Data fusion was defined in 1985 by the U.S. Joint Directors of Laboratories (JDL) and the model has been subject to later revisions. In this thesis MSDF will be defined identical to JDL's terminology of data fusion:

> Data fusion is the process of combining data or information to estimate or predict entity states [78].

This definition is rather general and is not limited only to the sensor systems available, but also to additional information and knowledge of the system evaluated together with the sensor data [7]. However, the idea of using several sources of information to define the current situation and the future prospects is not new. For centuries in medical science, using available information about the patient's current health status, the patient's health history and knowledge gained from other patients with similar symptoms are used to define a diagnosis of the condition of the patient and to predict the patient's future health condition. In physics, several data sources have been used to describe the behaviour of various systems, resulting in new knowledge about the system, and this knowledge is typically formulated as mathematical models. One such example is Newton's second law, relating the force $\mathbf{F}$ applied to an object to the mass m of the object and the acceleration $\mathbf{a}$, giving the relation $\mathbf{F} = m\mathbf{a}$.

In petroleum well drilling there is a large amount of data gathered from sensors prior to the drilling phase, during the actual drilling phase and after the drilling phase. Typically, all these data are presented to the operator and

the operator has to analyse the data manually. Since the amount of data is increasing as more sensor systems are developed and put into use, there is a need for a more automatic method to analyse and eventually evaluate the available data. If such a method is developed, then only the resulting analysis containing the required qualified information is presented to the operator. The operator can then use this qualified information as a basis for decision taking.

This chapter is divided into three sections. First the various sensor systems are described, the next section describes the knowledge gathered about drilling system contained in various kinds of systems models, and the last section presents some parameter estimation methods.

4.1 Sensors in drilling applications

During drilling operations it is important to measure various parameters that can be used to improve the understanding of the drilling process. This section presents some of the sensor systems and sensor transmission methods that are currently available. In addition new sensor technologies and sensor locations are suggested.

4.1.1 Sensor system terminology

The drilling industry has two different main terms that are used for data acquisition during the drilling operation. The term Logging-While-Drilling (LWD) was used to record and store the sensor data locally, and retrieve the data when the drilling tool has been pulled out from the well. The term Measurement-While-Drilling (MWD) was used for sensor data that are measured and sent to the surface systems for analysis while the drill bit is still in the well.

In the later years, as the data transmission technology has improved, the main difference between these two terminologies is now that the LWD is used for instruments that are used for estimation of the reservoir conditions and MWD is used for instruments that are closely related to the directional drilling operations [49].

Data acquisition for directional drilling

While drilling a well, it is important to know exactly where the drill bit is located. Therefore several sensors are placed at the drill bit to ensure that the planned well trajectory is followed. Several parameters are measured to ensure a correct drilling direction:

- wellbore geometry (inclination, azimuth),
- drilling system orientation (toolface),
- mechanical properties of the drilling process (rate of penetration).

The wellbore inclination and azimuth parameters are transferred to the surface in order to maintain directional control in real-time.

Data acquisition for reservoir characterization

Various methods have been examined for evaluation of reservoir properties based on information from sensors placed in the well. The physical measurement principles for reservoir characterization sensors are similar for both standard logging tools and LWD systems, and has been developed for conventional drilling [65].

In UBD, there is a need for new technologies. This includes both the physical measurement principles of the sensors and new sensor positions for estimating reservoir parameters. Several methods are based upon mud cake build-up, which is penetration of drilling fluid into the reservoir section of the well. One of the main targets in UBD is to avoid this mud cake build-up. Hence, currently available sensors are not necessarily capable of providing suitable data for reservoir characterization.

4.1.2 Data transmission methods

The data from the drilling sensors can be transferred to the surface using different telemetry principles [18]:

- Positive Pressure Pulse in Mud
- Continuous Pressure Wave in Mud
- Fluidic Vortex in Mud
- Acoustic Pulse along Drillstring
- Electromagnetic Signal using Drillstring as dipole
- Signal cable integrated in drillstring

The first four of these methods are based on using the drilling fluid as a medium for sending either pressure pulses or acoustic pulses. If there are compressible fluids in the well at a high gas/oil-ratio, such as during

UBD, then the electromagnetic signal telemetry method have been the only commercial method available. However, this method may experience some difficulties when used in deep wells.

Recently, a new approach for transmission of down-hole data has been tested and is becoming commercially available [30, 66]. A data cable is integrated into each pipe joint and has the possibility of transferring data not only from the bit but also from sensors mounted along the drillstring.

4.1.3 Currently available sensors

Several sensors are used to estimate the reservoir properties both during the drilling phase and after the drilling phase. The sensor systems are measuring different physical properties, and descriptions of various sensor systems can be found in [18, 68, 74]. Many of the sensing methods described in this section are based on penetration of drilling fluid into the reservoir section near the well, often referred to as mud cake build-up or skin damage [20].

The area of reservoir characterization while drilling is a huge area covering several disciplines from mechanical packaging of electronic circuits for high temperature and high pressure, to graphical presentation of computer generated images. Still, the same main physical properties are measured, such as the spontaneous-potential and the resistivity.

Since some of these measurements are based upon penetration of drilling fluid into the formation, problems will arise when analysing logging data from a well that has been drilled using UBD technology. Other and newer measuring techniques such as the NMR logging may be useful for UBD operations. This leads to a search for new methods when dealing with reservoir characterization during UBD.

Pressure and temperature

A key parameter during drilling operations is the BHP. The BHP data is transmitted to the surface, and is critical since the difference in pressure between the reservoir pore pressure and annulus BHP is relevant for the flow interaction between the well and the reservoir.

Temperature measurements are also available at the drill bit. The use of this parameter is mainly limited to monitor the operating condition of the drill bit, verifying that the drill bit temperature is within acceptable limits. The temperature is also an important parameter of the drilling fluid, since the viscosity and other fluid parameters are influenced by temperature. The temperatures of the drill bit and drilling fluid are mainly influenced by

the geothermal temperature, but the temperature may also increase due to friction when drilling in hard formations.

Multi-phase flow meters

Measuring the flow composition out of the well is important. This can either be done by measuring the levels in the separator which is placed after the choke, or by measuring the fluid components while the fluid is flowing in the pipe. Current research is now improving the physical measurement principles in separator systems [25]. There are commercially available flow meters for measuring the fluid components in a pipe, using a dual sensor system measuring the density and dielectric properties [69]. Methods for estimating the flow patterns are also emerging [24]. Mass flow meters such as the Coriolis mass flow meter can be used for measuring the total mass flow rate out of the well.

Acoustic emission

During drilling, particles are transported along the annulus. These particles coming in contact with the drillstring and the casing, will emit acoustic noise. Acoustic emission sensors can be placed downstream the choke valve, directly mounted on a pipe section [10]. Using cross-correlation analysis, the data from two acoustic emission sensors placed at two positions along a pipe can be used for calculating the flow rate of the particles.

Acoustic log

The acoustic log is based on measuring the transit time from an acoustic source to an acoustic receiver. The speed of sound is faster in the formation than in the drilling fluid. The transit time for the actual formation is compared with the transit time for a rock with no porosity and the transit time of the pore fluid. From these comparisons of transit times an indication of the porosity of the formation can be found.

Mud Log

The cuttings from the drilling process are transported to the surface together with the drilling fluid. The cuttings are analysed manually by geologists while drilling is performed. Several parameters are recorded, such as cuttings type and cuttings density. The mud is also analysed using gas chromatographs to examine if hydrocarbon gases are present.

Spontaneous-Potential log

The Spontaneous-Potential log (SP-log) is a method that can be used during standard overbalanced drilling. The principle is based on measuring the electric potential between an electrode at the surface and an electrode that is placed into the well. The SP-log gives different electric potential due to the difference in salinity between the drilling fluid and the reservoir fluid. The electric potential is due to the flow of ions from the more concentrated liquids to the less concentrated liquids. The potential is related to the permeability of the formation, since the drilling fluid has penetrated into the formation.

The measurements are measured relative to a baseline. When the measurements show negative recordings relative to the baseline, then this indicates a permeable formation. A positive measurement relative to the baseline occurs when the liquids in the reservoir has lower salinity than the drilling mud.

Resistivity log

A resistivity log gives the electrical resistivity of the formation. An oil filled reservoir has higher resistivity than an high-salinity water filled reservoir. Generally, three different types of resistivity logs exists:

- normal (conventional) log
- laterolog
- induction log

The normal log is measuring resistivity by setting up a potential between an electrode at the surface and an electrode at the end of the measuring device. The resistivity is measured between two other electrodes placed between the main electrodes. By changing the distance between the measuring electrodes, the resistivity at difference depth in the reservoir can be measured.

The laterolog uses a single current electrode, and two guard electrodes below and above the main electrode. The laterologs can measure the resistivity at different depths into the reservoir by changing the geometry of the central electrode and the guard electrodes.

The induction log has transmitter and receiver coils at each end of the measuring device. A signal is transmitted from the transmitter, and the receiver measures this signal. The distance between the transmitter and the receiver coils determines how far into the reservoir the resistivity is measured [1].

If the well is being drilled in overbalanced conditions, then some of the drilling mud penetrates into the permeable zones of the reservoir. Depending on the permeability and other reservoir parameters of the reservoir zone, the drilling mud continues to migrate further into the reservoir zone. Since the drilling mud has different electrical properties than the reservoir fluids, then the resistivity close to the well is different to the resistivity further away from the well where there are only reservoir fluids. If deep and shallow resistivity measurements were performed, then combination of the measurements could be used to locate a permeable zone.

Natural radioactivity log

The natural radioactivity log is used to measure the natural radioactivity of the sediments in the reservoir. The different sediments emit different radioactivity. Since this type of measurement is not dependent on mud cake build-up, it could be used in UBD.

Neutron log

A neutron source is emitting neutrons into the formation, releasing gamma rays that are emitted from the reservoir relative to the hydrogen content. There is hydrogen in all formation fluids such as oil and water, but not in the formation stone itself. The neutron log contains information about the porosity of the formation.

Density log

The density log is based on measurements of gamma rays from the formation. A gamma ray source emits gamma rays into the formation. Gamma rays returning from the reservoir give an indication of the electron density of the atoms in the reservoir, leading to information about the formation density.

The density log only registers the density of the formation close to the well. In a porous part of the formation, the drilling fluid is penetrating into the formation, and the porosity of the formation is a relationship between the formation density, the recorded density and the drilling fluid density.

Nuclear Magnetic Resonance log

An NMR log can be used for measuring porosity in the formation. The measuring principle is based on applying magnetic field oscillations in the well. A strong magnetic field is applied to the sides of the well, and the hydrogen nucleus reacts with this field. The time used for the hydrogen atom to align

to the magnetic field is measured, in addition to the relaxation time when the magnetic field is turned off. Fast relaxation indicates large pores, and slow relaxation time indicates small pores. The NMR measurements can be combined with the neutron density log to evaluate the reservoir permeability [49]. Application for UBD could be useful since the technology is not dependent on penetration of drilling fluids into the reservoir.

Dielectric log

The dielectric constant is different for water (50-80), for oil (2.0-2.3) and gas (1.0). When the dielectric constant is measured along the side of the well, this gives an indication of the type of reservoir fluid.

4.1.4 Suggested sensor designs

Since several of existing sensor systems for analysing the reservoir pressure are based on invasion of drilling fluid into the formation, new sensor systems should be evaluated. Both UBD operations and well pressure testing operations result in influx of reservoir fluid from the formation. It should be evaluated if methods used in well pressure testing can be used in UBD. Bear in mind that the sensors also have to sustain the environment with pressures typically between 100-300 bar and temperatures typically between 80 °C-200 °C.

Non-intrusive annulus flowmeter

One major data source when estimating reservoir parameters is the flow rate of reservoir fluids. In a production well the influx from the reservoir can be measured using down-hole flow measurement equipment placed in the production liner [17]. During UBD operation it is difficult to measure the flow rate directly, but indirect methods could be used.

The local flow rate along the annulus outside the drillstring may vary. This is because the reservoir influx has a transient decaying flow rate dependent on the time since the reservoir were drilled into. In addition, changes in the well pressure also influence the reservoir influx. Hence, the flow rate has to be measured on several locations. Installing several flow sensors for measuring annulus flow might not be technically or economically feasible. However, measuring the local flow at the casing shoe could be a possible future sensor location. Fig. 4.1 presents a suggested design for such a flow sensor system.

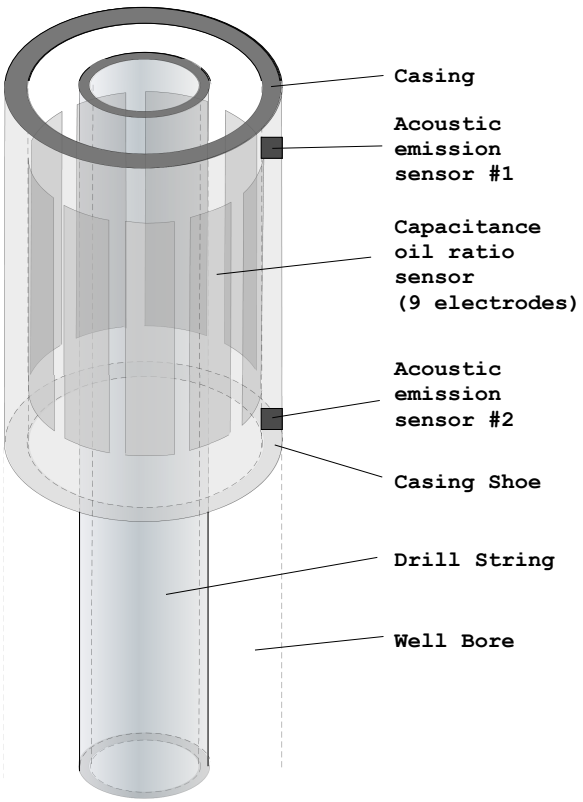

Figure 4.1: Suggested design of the non-intrusive annulus flowmeter using both capacitance electrodes and acoustic emission sensors

When estimating flow based upon measuring another physical parameter, several methods can be used. For measuring local flow, an acoustic emission sensor can be placed at two locations close to each other, and a cross correlation algorithm can be used to estimate the time lag between the signals measured. The time lag and the distance between the sensors and the flow area can then be used to calculate the local fluid volume flow rate [54]. Capacitance electrodes could also be used for measuring the oil ratio in the total flow, adapting to existing capacitance flow sensors [25].

Sensor arrays

The influx of reservoir fluids will affect the annulus pressure. The pressure measured in annulus can be used to estimate the reservoir parameters [85, 86, 87]. Introducing temperature measurements could in the future be useful for estimating reservoir parameters while drilling.

A temperature array could measure the thermal difference between the circulation fluid and the reservoir fluid. The temperature after mixing of the fluids is dependent on the mass flow rate, and will therefore contain information about the volume flow rate, when the densities of the fluids are known. The temperatures of the reservoir fluids have geothermal temperature, and the drilling fluid is circulated from the surface system. The temperature of the drilling fluid is increased while flowing down to the drill bit, but the drilling fluid has still lower temperature than the reservoir fluids coming into the well annulus. In the annulus the drilling fluids and the reservoir fluids are mixed, and transported together up to the surface.

The temperature gradient along the annulus could be measured along the outside of the drillstring using single temperature sensitive fibre optical cable with Bragg-grating [38]. Such temperature sensors arrays are currently developed for production wells [90].

In Fig. 4.2 a future sensor array layout is shown. The temperature and pressure sensors could be placed along the drillstring, and measure the pressure and temperature variations at positions within the reservoir zone of the well.

4.2 Modelling fluids

Knowledge about how various parameters such as pressure, temperature and flow rate interact in various fluid systems has been implemented in several mathematical models. For simple model approach the buoyancy laws can be used, whereas the Navier-Stokes equations (see e.g. [91]) can be used to

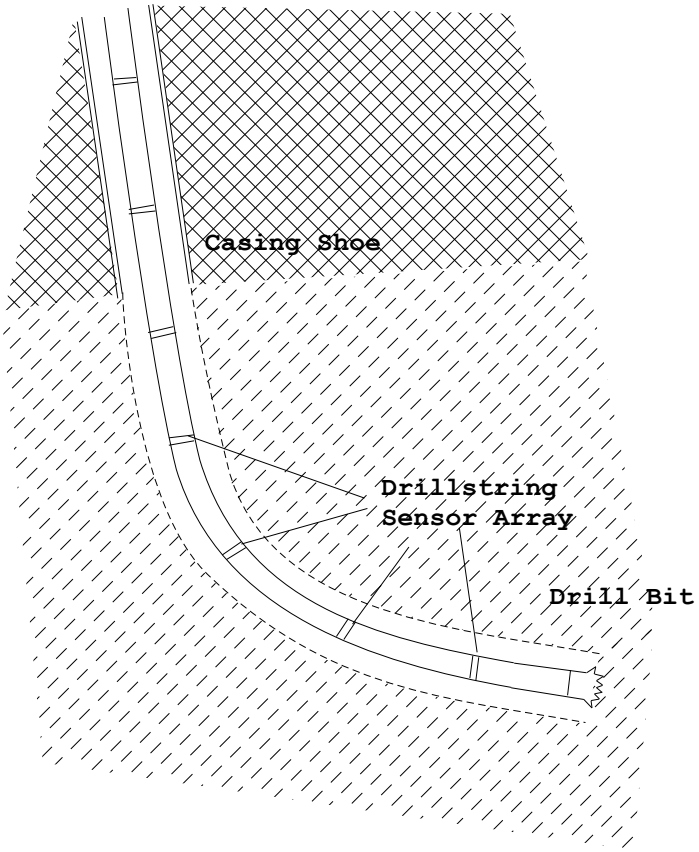

Figure 4.2: Suggested design of the temperature and pressure sensor array placed along the drillstring.

describe the non-linear behaviour of dynamic fluid flow. Still with today's computing power it takes a long time to calculate the behaviour of a dynamic fluid system using the Navier-Stokes equations. However, between these two modelling efforts of describing fluid effects, several methods exist that are able to describe the behaviour of a dynamic fluid system sufficiently accurately in real-time.

As an alternative to the standard modelling efforts, using neural networks as a function approximation could be implemented and used to describe various parameters. Using a given set of pressures, temperatures and flow rates, a neural network could be trained to calculate the behaviour of the dynamic fluid.

However, in an MSDF perspective, to include the knowledge from process models is crucial for the fusion of the available data from the various sensors [7]. When modelling UBD, the BHP is the most important parameter to be estimated correctly. But, since this parameter is very dependent on other parameters such as the density and friction pressure loss, these modelling efforts can be complex. This is especially true when the underbalanced conditions in the well are achieved by injecting gas. This results in two-phase flow conditions, which add even more to the complexity of dynamic models of the well fluid flow.

The well and reservoir system can be represented by a discrete explicit scheme given by

$$\mathbf{x}_k = f\left[\mathbf{x}_{k-1}, \theta\right] \tag{4.1}$$

$$\mathbf{y}_k = h\left[\mathbf{x}_k\right] \tag{4.2}$$

where $f[\cdot]$ is the function for calculating the current state vector $\mathbf{x}_k$ based on the previous state vector $\mathbf{x}_{k-1}$, θ is some uncertain model parameters, typically reservoir pressure or reservoir permeability. $h[\cdot]$ is the function for calculating the current sensor values $\mathbf{y}_k$ based on the current state vector.

This section presents three different modelling efforts for describing the dynamic pressure variations in UBD. First section describes a model with ordinary differential equations with time as the differential operator. The second section describes a more detailed model where the spatial dynamics in the well are calculated using partial differential equations using both the depth of the well and the time as differential operators. In the third section a neural network approach is discussed.

4.2.1 Low-order dynamic state models

When modelling fluid flow during drilling, it is assumed that the flow pattern in the drillstring is uniform along the whole length of the drillstring, and that

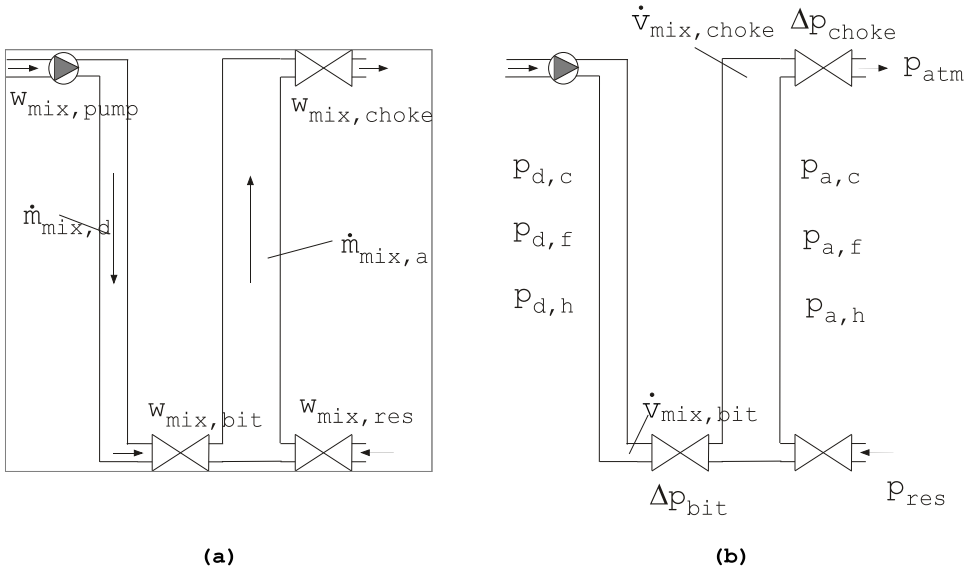

Figure 4.3: The mass balance of the well (a), and the pressure balance of the well (b).

the flow pattern in the annulus is uniform in the whole length of the annulus. Therefore, the well can be divided into two compartments with different dynamics, the drillstring and the annulus [58]. The interconnection between these two compartments is modelled using mass balances and pressure balances. Fig. 4.3 shows the diagrams of the mass flows and the pressures in the well.

Due to the two-phase flow, a separate mass balance for the gas and the liquid are defined. The mass balances for the fluids in the drillstring are given by:

$$\frac{d}{dt}m_{g,d} = w_{g,pump} - w_{g,bit}, \quad m_{g,d}(0) = m_{0,g,d} \tag{4.3}$$

$$\frac{d}{dt}m_{l,d} = w_{l,pump} - w_{l,bit}, \quad m_{l,d}(0) = m_{0,l,d} \tag{4.4}$$

where $w_{\star,bit}$ is the mass flow of gas and liquid at the drill bit, respectively. The mass balance equations for the annulus are given by:

$$\frac{d}{dt}m_{g,a} = w_{g,bit} + w_{g,res} - w_{g,choke}, \quad m_{g,a}(0) = m_{0,g,a} \tag{4.5}$$

$$\frac{d}{dt}m_{l,a} = w_{l,bit} + w_{l,res} - w_{l,choke}, \quad m_{l,a}(0) = m_{0,l,a} \tag{4.6}$$

where $w_{\star,res}$ is the mass flow of gas or liquid at the reservoir, and $w_{\star,choke}$ is the mass flow of gas or liquid at the exiting choke valve.

In addition to the mass balances, a pressure balance needs to be set up. This is because the friction pressure in the well is strongly related to the flow rates in the well, causing unsteady flow conditions [51]. The pressure balance is set up at the drill bit at the bottom of the well, and at the choke valve at the exit of the well. The pressure balance equations are given by

$$\begin{aligned} \frac{d}{dt}v_{mix,bit} &= \frac{1}{\rho_{mix,d}L}\left(p_{d,c}+p_{d,g}-p_{d,f}-\Delta p_{bit}-p_{a,c}-p_{a,g}-p_{a,f}\right) \quad (4.7)\\ v_{mix,bit}(0) &= 0 \\ \frac{d}{dt}v_{mix,choke} &= \frac{1}{\rho_{mix,a}L}\left(p_{a,c}-\Delta p_{choke}-p_{atm}\right), \quad (4.8)\\ v_{mix,choke}(0) &= 0 \end{aligned}$$

where $\rho_{mix,\star}$ is the mixture density of the fluid in the drillstring or annulus and $p_{\star,\star}$ is pressure and L is well length. The subscript d denotes parameters related to the drillstring, and subscript a denotes parameters related to the annulus. The subscript c denotes the compression pressure, subscript g denotes the gravitational pressure and subscript f denotes the frictional pressure loss. Further, Δp_{bit} is the pressure loss over the bit, and Δp_{choke} is the pressure loss over the choke. $v_{mix,bit}$ is the mixture flow velocity before the drill bit flow restriction and $v_{mix,choke}$ is the mixture flow velocity before the choke valve. p_{atm} is the atmospheric pressure.

In addition the mass balance and the pressure balance, the length of the well is also increasing as a function of time. The depth of the well also influences the well pressure, and therefore the well length L is chosen as a state in the dynamical system, given by

$$\frac{d}{dt}L = v_d \quad L(0) = L_0 \quad (4.9)$$

where v_d is the vertical drilling rate, and L_0 is the initial well length.

A total of 7 states are therefore defining the dynamics of the well during drilling. The closure relations between masses, flow rates and pressures are further described in [59]. This type of simple modelling methodology can be used for design and analysis of a control system for the pressure in the well. For a more accurate prediction of the mass flow along the well, a more detailed model should be used.

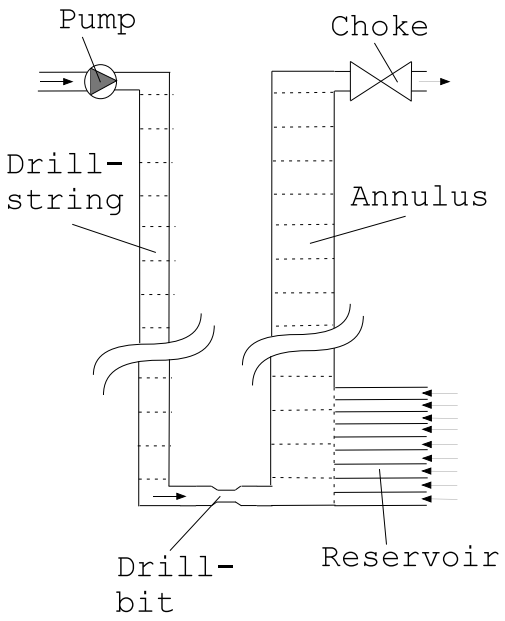

Figure 4.4: Spatial discretization of the drillstring, the annulus and the annulus-reservoir interaction

4.2.2 Detailed flow modelling

The research within dynamic well modelling focuses on methods for accurately describing the fluid flow along a well. The Navier-Stokes equations are used as a basis for the description, where the well is divided into small boxes along the drillstring and the annulus. Fig. 4.4 shows the discretization along the well and reservoir.

In the conservation equations for the mass balances for gas and liquid, the mass transfer between the phases are neglected. The mass balance for each phase is

$$\frac{\partial}{\partial t}\left(\rho_g \alpha_g\right) + \frac{\partial}{\partial z}\left(\rho_g \alpha_g v_g\right) = 0 \tag{4.10}$$

$$\frac{\partial}{\partial t}\left(\rho_l \alpha_l\right) + \frac{\partial}{\partial z}\left(\rho_l \alpha_l v_l\right) = 0 \tag{4.11}$$

where $\rho_\star$ is the fluid density, $v_\star$ is the phase velocity and $\alpha_\star$ is the void fraction.

The momentum equations for each phase are added together, which results in the drift-flux formulation. The drift-flux formulation is a simplified

momentum balance equation for the mixture, given by

$$\begin{aligned} & \frac{\partial}{\partial t}\left(\rho_l \alpha_l v_l + \rho_g \alpha_g v_g\right) \\ + & \frac{\partial}{\partial z}\left(\rho_l \alpha_l v_l^2 + \rho_g \alpha_g v_g^2 + p\right) \;=\; -\frac{d}{dz} p_f \\ & \qquad\qquad - \left(\rho_l \alpha_l + \rho_g \alpha_g\right) g \sin\theta \end{aligned} \tag{4.12}$$

where p is the pressure, p_f is the frictional pressure component caused by both the viscous effects of the fluid and the wall shear stress factor and θ is the angle between the gravity direction and the well trajectory direction. The closure relations are further described in [41].

A numerical scheme has been developed over several years [28, 82, 92], and verified with several experimental tests [42, 43]. The well inflow from the reservoir is defined using the equations from the well pressure test at constant rate given in [11]. The reservoir model and the well model are combined by dividing the reservoir into several small segments, each having contact with the well [85].

Since this type of model calculates the behaviour of the fluids in more detail, the model will be more accurate. The mass balance for each box is calculated along with the pressure balance, giving mass for each phase and velocity of the mixture as well as the pressure in the box. This results in a high-order state vector for a model with several boxes. Nevertheless, due to increased computational power, the model state can be calculated about 100 times faster than real-time on a standard Intel Pentium(III) 1GHz CPU.

4.2.3 Model approximation using neural nets

An artificial neural network is a calculation scheme based on the behaviour of real neurons in the human brain [39]. An artificial neural network can have various structures depending on the applications. A feed-forward neural network can be calculated very fast. In the effort of modelling a physical system, a feed-forward neural network can be used as a model approximation. Initially the feed-forward neural network is trained using data from the model that is to be approximated. When the training is completed, the neural network can be used instead of the model, as a fairly good approximation and at a lower computational cost. According to [21], most functions can be approximated using a two-layer network using neurons with a sigmoid function in the first layer and neurons with a linear function in the second layer.

Feed-forward Neural network

The output a of a single artificial neuron can be described as

$$a = f(n), n = \mathbf{W}\mathbf{p} + b \tag{4.13}$$

where f is the neuron transfer function, n is the input of the neuron transfer function, $\mathbf{W}$ is the weight matrix, $\mathbf{p}$ as the input vector and b as the bias. The neuron can be organised in layers, and each layer can consist of several neurons. The total neural network consists of several layers. The neuron transfer function can be of different types, such as log-sigmoid function given by

$$a = \frac{1}{1 + e^{-n}} \tag{4.14}$$

or the saturating linear function given by

$$\begin{aligned} a &= 0, n < 0 \\ a &= n, 0 \leq n \leq 1 \\ a &= 1, n > 1 \end{aligned} \tag{4.15}$$

The weight matrix, $\mathbf{W}$, can be adjusted according to the function or data that is to be approximated. This adjustment process of the weights is called training. A feed-forward network can be trained using the back-propagation algorithm or other algorithms. A data set with a certain amount of inputs with known outputs is used as a training set.

Examples

A simple example for function approximation is given below, and the example is implemented using MATLAB [21, 22]. The inflow from the reservoir during UBD can be described using Eq. (3.11), which is used to generate the "true" measurements. A three layer neural network is used. The first layer has 6 neurons and a log-sigmoid transfer function. The second layer has 3 neurons and a log-sigmoid transfer function. The output layer is a single neuron with a linear transfer function. The training is done using the MATLAB function `trainbr`, which is using a implementation of the Levenberg-Marquardt optimisation algorithm. The results from the simulations are shown in Fig. 4.5.

The network gives a good approximation of the function, and this corresponds to the results found in literature [21]. During UBD, the real inflow from the reservoir is unknown, and models must be used to train the network. However, both flow models described in the previous sections are calculated

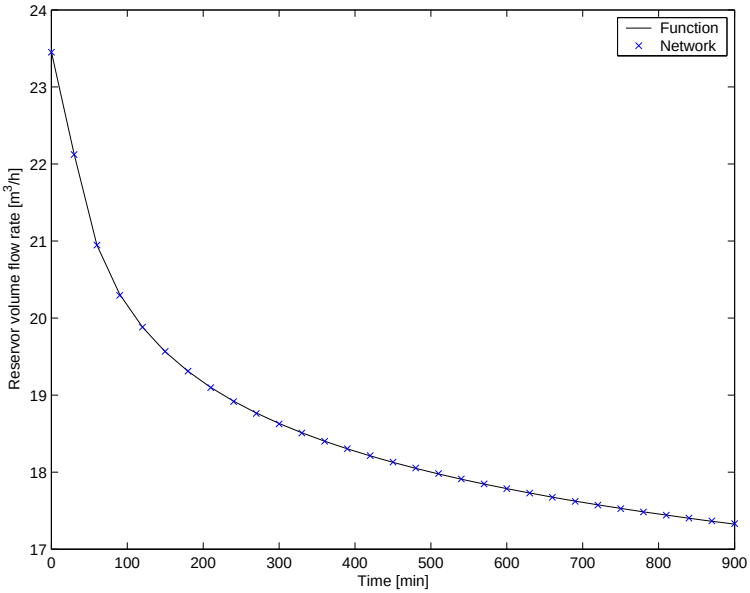

Figure 4.5: Feed-forward neural network as a function approximation of the transient reservoir inflow function trained using the Levenberg-Marquardt optimization algorithm.

faster than real-time, so the need for improving the calculation time is not critical.

Neural networks has been used with success within other fields of petroleum engineering. In [12] the aim is to define well trajectories in a reservoir. A complex reservoir model is used to calculate the reservoir utilization using different positions and lengths of the wells. The results are used to train a feed-forward neural network, since the neural network is faster than the reservoir model. The neural network is then used in an optimisation algorithm to search for the best selection of wells in the effort of optimising the reservoir utilization.

4.3 Data fusion methods

This section focuses on how to use and combine the various data from the sensors together with the knowledge gained from the models, resulting in more qualified information.

The most intuitive method when trying to estimate parameters is to combine data from different sensors using simple relations between the actual parameters that are measured. This method is described in the first section.

History matching is based on using historical measured sensor data sets and trying to fit simulated data sets generated by a model of the system to these sensor data sets. The model and the data can be fitted by searching for the minimum error between the measured data and the equivalent data calculated using the model. When using history matching, all the measurements are processed in the algorithm after the operation is finished. To search for the minimum solution of the least squares problem then the Levenberg-Marquardt algorithm [53] is used, which is a variation of the Newton search algorithm.

However, during control of a process, there is a need for estimating the parameters while the process is actually running. In such cases, data assimilation algorithms can be used. Such algorithms can update the model parameters when the measurements are available for processing. The synchronising of data sources when evaluating sensor data received at different points in time should be take into account when implementing the algorithms [5].

The model will contain model errors and the measurements will have measurement noise, which should be accounted for when comparing the model calculations with the measurement data from the sensors. An extended Kalman filter (EKF) could be used, but the method is time consuming when having high-order state-vectors since the EKF requires numerical differentiation. Instead, two variations of the Kalman-filter are tested, the ensemble Kalman filter (EnKF) and the unscented Kalman-filter (UKF) [16, 33].

This section presents various methods for estimating unknown parameters using simple sensor data combination techniques, neural net classification, history matching and data assimilation.

4.3.1 Combining sensor information

All the various logs used for reservoir characterization described in Section 4.1.3 give some information if they are used separately. However, if the data logs are used together, additional information can be extracted.

Combining SP-log and Resistivity log

By combining the SP-log and the resistivity log, the water saturation of the porous parts for the formation can be found (see e.g. [74]). The water saturation S_w is calculated using

$$S_w = \frac{(R_{xo}/R_t)^{5/8}}{R_{mf}/R_w} \tag{4.16}$$

where R_{xo} is resistivity measured using a shallow resistivity log, R_t is the resistivity measured using a deep resistivity log, R_{mf} is the resistivity of the drilling mud, and R_w is found from the SP log.

Combining porosity logs

By combining the porosity logs, more accurate values of the porosity can be found, and useful additional information can be extracted. As an example, when measuring the porosity using a neutron log and a density log, then the content of gas in the formation will influence the measurements. This leads to a method to decide if there are gas zones in a limestone reservoir [49].

Methods used for well testing

When an oil well is being drilled, and later during the production phase of the oil well, the properties of the reservoir are evaluated using a well testing procedure. When performing a well test, the well is being shut in, and the well pressure at the reservoir section is increased until a steady state is reached. Then the well is opened, and the volume rate from the well is being kept constant while the pressure is measured. This is called the constant terminal rate test, and the relation between the differential pressure and the flow rates is found by solving Eq. (3.11).

4.3.2 Classification using neural nets

A neural net has a good capability to be used as classifier for a pattern recognition problem. The main problem for the neural net, is that it needs information to be able to train the network. To train the network, a model can be used. An inverse model of the system can then be designed by training the neural net using the output of the forward model as input, and the input of the forward model as output. An example for using a neural net as a classifier is given in Chapter 5.

4.3.3 History matching

The idea of history matching is to tune a model such that the state and parameters of the model match with previous measured data. One effort is to focus on the unknown parameters of the model. The minimization problem for the time series can be defined as a least squares problem presented as

$$S(\theta) = \sum_{k=1}^{n} \left[\mathbf{r}_k(\theta)\right]^2 \tag{4.17}$$

$$\mathbf{r}_k(\theta) = \mathbf{y}_k^m - \mathbf{y}_k^c \tag{4.18}$$

where the cost criterion S is defined by a squared sum of differences $\mathbf{r}_k$. The array of parameters θ is selected as unknowns to the model, $\mathbf{y}_k^m$ is the measured sensor data from the process and $\mathbf{y}_k^c$ is the calculated sensor value based on a model derived from (4.1)-(4.2), k is the current timestep and n is the total number of time steps.

History matching using Levenberg-Marquardt algorithm (LM)

When solving linear least squares problems such as given by Eq.(4.17) then the Newton algorithm can be used [73]. The Newton algorithm is an iterative scheme which uses an initial guess of the parameter vector θ^i, to search for the true parameter vector θ^*. The Newton algorithm is given by

$$\theta^{i+1} = \theta^i + \delta^i \tag{4.19}$$

$$\delta^i = -\left(\mathbf{J}^{iT}\mathbf{J}^i + \mathbf{A}^i\right)^{-1}\mathbf{J}^{iT}\mathbf{r}^i \tag{4.20}$$

$$\mathbf{J}^i = \frac{\partial \mathbf{r}^i}{\partial \theta^{iT}} \tag{4.21}$$

$$\mathbf{A}^i = \sum_{j=1}^{p} r_j{}^i(\theta)\,\frac{\partial^2 r_j{}^i(\theta)}{\partial\theta^i \partial\theta^{iT}} \tag{4.22}$$

where i is the search step, j is the measurement index and p is the number of measurements.

Since calculating the Hessian matrix $\mathbf{A}$ is computationally intensive, then the Gauss-Newton algorithm can be used if $\mathbf{A}$ is small compared with $\mathbf{J^T J}$. The Gauss-Newton algorithm is equivalent to the Newton algorithm when $\mathbf{A}$ is ignored, giving

$$\delta^i = -\left(\mathbf{J}^{iT}\mathbf{J}^i\right)^{-1}\mathbf{J}^{iT}\mathbf{r}^i \tag{4.23}$$

For nonlinear problems, where $\mathbf{J}^{iT}\mathbf{J}^i$ can be singular or ill-conditioned, then Eq. (4.23) can be modified to

$$\delta^i = -\left(\mathbf{J}^{iT}\mathbf{J}^i + \lambda^i\mathbf{D}^i\right)^{-1}\mathbf{J}^{iT}\mathbf{r}^i \tag{4.24}$$

where λ^i is a scalar value known as the Levenberg-Marquardt parameter, and $\mathbf{D}^i$ is a diagonal matrix with positive elements along the diagonal. In the implementation of the Levenberg-Marquardt algorithm, the calculation of the inverse of $\mathbf{J}^{iT}\mathbf{J}^i + \eta^i\mathbf{D}^i$ is not performed, but the step δ^i is found by solving the least squares problem

$$\min_{\delta} \left\| \begin{pmatrix} \mathbf{r}^i \\ \mathbf{0} \end{pmatrix} + \begin{pmatrix} \mathbf{J}^i \\ (\lambda^i \mathbf{D}^i)^{1/2} \end{pmatrix} \delta \right\|^2 \tag{4.25}$$

If λ^i is close to zero, the algorithm will have a step nearly in the Gauss-Newton direction. If $\lambda^i \to \infty$, then the steepest-descent direction is chosen (see e.g. [47]), but the step length will tend to zero.

A modification of the Levenberg-Marquardt algorithm to include constraints of the parameters θ^i such as

$$\theta_{min} < \theta^i < \theta_{max} \tag{4.26}$$

has been implemented as suggested in [19].

History matching using genetic algorithms (GA)

Genetic algorithms is an optimization method that origins from the evolution theory of survival of the fittest. A cost criterion such as given in (4.17) is minimized using a special search algorithm [7, 9, 39].

The parameter set θ is converted to a binary representation θ_b represented as

$$\theta_b = B(\theta) \tag{4.27}$$
$$\theta = B^{-1}(\theta_b) \tag{4.28}$$

where $B(\cdot)$ is used for generating the binary representation, and $B(\cdot)^{-1}$ is generating the parameter based on the binary representation. The terminology in the genetic algorithm is also adopted from the biology, and θ_b is denoted as the *gene* representation of the θ. Genetic algorithms have the ability of finding a global maximum in a search environment where there are several local maximum values. In [6] a genetic algorithm was used to estimate the reservoir parameters. However, if the number of generations is too high, then the algorithm can be computationally costly, close to a Monte-Carlo approach.

History matching using simulated annealing algorithm (SA)

A third approach for finding the optimal value in (4.17) is to use the method of simulated annealing [7]. The algorithm simulates the annealing of a material. If a material is cooled slowly, then the material will form crystals, and then settle at a minimum energy state. The terminology used in the algorithm is taken from this annealing process.

In [52, 63] the simulated annealing was compared with gradient based methods such as the Levenberg-Marquardt algorithm, and the simulated annealing method was found to be too slow.

In the current work, focus have been on using the Levenberg-Marquardt algorithm for history matching.

4.3.4 Data assimilation using Kalman-filters

There is a need for estimating unknown parameters such as reservoir pressure and permeability during the drilling operations. The various Kalman filters give the possibility to estimate these with the minimum variance of the estimation error, by augmenting the state vector with a Markov process description of the parameters [8]. Based on Eqs. (4.1)-(4.2) a revised model can be defined by

$$\mathbf{x}_k = f\left[\mathbf{x}_{k-1}, \theta\right] + \mathbf{v}_k \tag{4.29}$$

$$\mathbf{y}_k = h\left[\mathbf{x}_k\right] + \mathbf{w}_k \tag{4.30}$$

where $\mathbf{v}_k$ is the process noise and model error, and $\mathbf{w}_k$ is the measurement noise. For estimating the unknown process parameters in the model, the measurements can be used to update the model parameters in real-time. When estimating model parameters, then the model state is augmented with the model parameters. The original Kalman filter was developed for linear models. For nonlinear models there have been developed various alternatives [8]. This section will describe the extended Kalman Filter, the ensemble Kalman Filter and the unscented Kalman Filter.

The extended Kalman-filter (EKF)

The discrete extended Kalman filter with an augmented state vector $\chi = [\mathbf{x}, \theta]$ consisting of the original state vector x and the unknown model parameters θ, uses a linearization of the state function $f[\cdot]$ and the measurement function $h[\cdot]$ given by

$$\mathbf{F}_k = \frac{\partial f[\chi]}{\partial \chi}|_{\chi_k} \tag{4.31}$$

$$\mathbf{H}_k = \frac{\partial h[\chi]}{\partial \chi}|_{\chi_k} \tag{4.32}$$

where k is the current time step.

The extended Kalman filter uses the augmented linearized model to calculate the estimation error covariance matrix $\mathbf{P}_k$. The current time step

is denoted using subscript k and the next time step is denoted using subscript $k+1$. The covariance matrix for the model error is $\mathbf{Q}_k$, giving $\mathbf{v}_k \sim \mathbf{N}(0, \mathbf{Q}_k)$ and the covariance matrix for the measurement noise is $\mathbf{R}_k$, giving $\mathbf{v}_k \sim \mathbf{N}(0, \mathbf{R}_k)$, and $\mathbf{N}(\mu, \sigma^2)$ is the normal probability distribution with mean μ and variance σ^2. The covariance matrixes are assumed to be non-correlated.

The notation used here is based on the notation in [16], but is slightly modified with reference to the control system literature (see e.g. [2, 3, 23, 33, 76]). The term *forecast* with superscript f is used instead of the term *apriori* for the calculations at the current time step before the measurements are included in the filter, and the term *analyzed* with superscript a is used instead of the term *aposteriori* for the calculations at the current time step after the measurements are included in the filter. The following equations shows the extended Kalman filter

$$\begin{aligned}
\chi_k^f &= f[\chi_{k-1}^a] && (4.33)\\
\mathbf{P}_k^f &= \mathbf{F}_{k-1}\mathbf{P}_{k-1}^a\mathbf{F}_{k-1} + \mathbf{Q}_k && (4.34)\\
\mathbf{K}_k &= \mathbf{P}_k^f\mathbf{H}_k^T\left(\mathbf{H}_k\mathbf{P}_k^f\mathbf{H}_k^T + \mathbf{R_k}\right)^{-1} && (4.35)\\
\chi_k^a &= \chi_k^f + \mathbf{K}_k\left(\mathbf{y}_k^m - \mathbf{H}_k\chi_k^f\right) && (4.36)\\
\mathbf{P}_k^a &= \mathbf{P}_k^f - \mathbf{K}_k\mathbf{H}_k\mathbf{P}_k^f && (4.37)
\end{aligned}$$

where y_k^m is the measurement which is equivalent to

$$\mathbf{y}_k^m = h[\chi_k^t] + \mathbf{w}_k \qquad (4.38)$$

where χ_k^t is the unknown true state.

The gradient matrix found in (4.31)-(4.32) are computational costly, and especial for models with a large number of states. Other Kalman filter methods are therefore investigated.

The ensemble Kalman filter (EnKF)

The ensemble Kalman Filter was introduced in [15]. The main idea behind the method is that an ensemble of n model instances is calculated at each time step and the result from the n forecasts is used to calculate the estimation error statistics. The description of the ensemble Kalman Filter follows the presentation given in [16], however with some changes in the notation. The initial ensemble $\chi_{initial}^{(j)}$ is randomly selected using a normal probability

distribution with an assumed initial covariance $\mathbf{Q}_0$, giving $\mathbf{v}_0 \sim \mathbf{N}(0, \mathbf{Q}_0)$, using

$$\chi_{initial}^{(j)} = \chi_{initial} + \mathbf{v}_0^{(j)} \tag{4.39}$$

where $\chi_{initial}$ is the assumed initial mean when the filter is started, and the notation using (j) as upper index is a term for ensemble member j. In the following notation the measurement function in (4.30) is replaced by the linear operator $\mathbf{H}$ using

$$\mathbf{y}_k = \mathbf{H}\chi_k + \mathbf{w}_k \tag{4.40}$$

The ensemble of model states is represented by

$$\begin{array}{rclrcl} \chi_k^{f(0)} & = & f[\chi_{k-1}^{a(0)}], & \chi_0^{a(0)} & = & \chi_{initial}^{(0)} \\ \chi_k^{f(1)} & = & f[\chi_{k-1}^{a(1)}], & \chi_0^{a(1)} & = & \chi_{initial}^{(1)} \\ \vdots & \vdots & \vdots & \vdots & \vdots & \vdots \\ \chi_k^{f(n)} & = & f[\chi_{k-1}^{a(n)}], & \chi_0^{a(n)} & = & \chi_{initial}^{(n)} \end{array} \tag{4.41}$$

where n is the number of ensemble members, k is the time index, a is the analysed state and f is the forecasted state. The forecasted ensemble state is used to calculate the mean of the forecasted state vector using

$$\overline{\chi_k^f} = \frac{1}{n}\sum_{j=0}^{n} \chi_k^{f(j)} \tag{4.42}$$

The forecasted covariance of the model error $\mathbf{P}_k^f$, is found using the definition of covariance, based on the forecasted model states of the ensemble members using

$$\mathbf{P}_k^f = \overline{(\chi_k^f - \overline{\chi_k^f})(\chi_k^f - \overline{\chi_k^f})^T} \tag{4.43}$$

The measurement vector $\mathbf{y}_k^m$ is perturbed for each ensemble member with the measurement error $\mathbf{w}_k$ to ensure that the measurement has the covariance $\mathbf{R}_k$ using

$$\mathbf{y}_k^{m(j)} = \mathbf{y}_k^m + \mathbf{w}_k^{(j)} \tag{4.44}$$

$$\mathbf{R}_k = \overline{\mathbf{w}_k \mathbf{w}_k^T} \tag{4.45}$$

The analysis equations for the ensemble Kalman Filter is then

$$\mathbf{K}_k = \mathbf{P}_k^f \mathbf{H}^T \left(\mathbf{H}\mathbf{P}_k^f \mathbf{H}^T + \mathbf{R}_k\right)^{-1} \tag{4.46}$$

$$\chi_k^{a(j)} = \chi_k^{f(j)} + \mathbf{K}_k \left(\mathbf{y}_k^{m(j)} - \mathbf{H}\chi_k^{f(j)}\right) \tag{4.47}$$

$$\overline{\chi_k^a} = \frac{1}{n}\sum_{j=0}^{n} \chi_k^{a(j)} \tag{4.48}$$

$$\mathbf{P}_k^a = \mathbf{P}_k^f - \mathbf{K}_k \mathbf{H} \mathbf{P}_k^f. \tag{4.49}$$

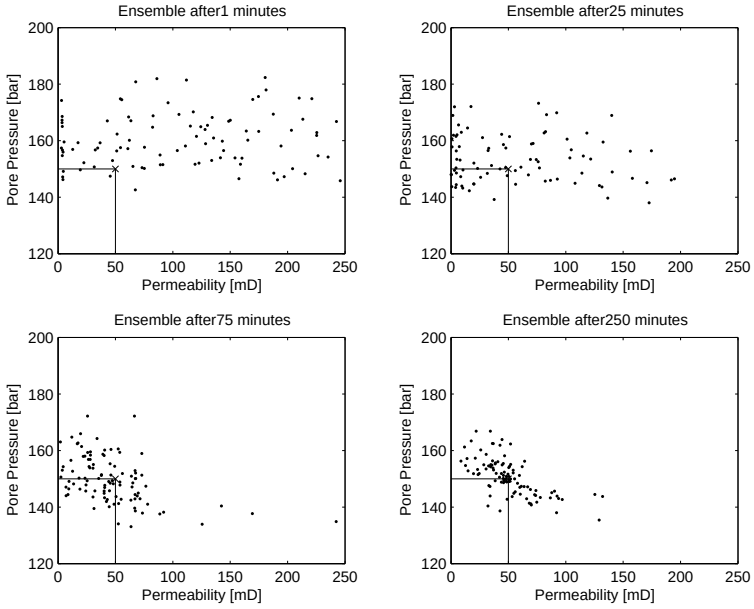

Figure 4.6: Distribution of the reservoir pore pressure and permeability in an ensemble at various time steps when estimating the reservoir parameters during drilling.

The ensemble Kalman Filter algorithm is equivalent to the Kalman Filter for linear system. For nonlinear systems, the extended Kalman filter uses a linear approximation for the nonlinear terms, using the gradient operation, and neglecting the higher order terms. The ensemble Kalman filter include these terms using the nonlinear model directly, and no need for linearization are needed [16].

In the current work, the ensemble Kalman Filter has been used for estimation of the reservoir parameters in a detailed well-reservoir model. To illustrate how the ensemble Kalman Filter converges, the reservoir parameter distribution from Example 3 in [59] is shown in Fig. 4.6. The two parameters, pore pressure and permeability, are plotted after 1 minute, after 25 minutes, after 75 minutes and after 250 minutes.

The unscented Kalman-filter (UKF)

The unscented Kalman Filter (UKF) is another derivative-free Kalman filter for nonlinear estimation [32, 33, 34, 35]. Similar to the EnKF, the UKF does not use a linearization of the model to calculate the estimation error covariance matrix, but instead it tries to approximate this matrix by introducing sample points. The nonlinear model is applied to a set of state

vectors points, called sigma points. These sigma points are used to calculate the probability distribution of the estimation error. This description of the unscented Kalman filter follows the presentation in [83, 89], where the unscented Kalman filter is used for parameter estimation. The notation has been changed slightly for comparison with the other Kalman filters in this section.

Initially, the augmented state vector is assumed to be $\chi_0^a = [\mathbf{x}_0^a, \theta_0^a]$, with an estimation error covariance matrix $\mathbf{P}_0^a$. The sigma points are calculated using a design parameter λ. The design parameter can be defined by

$$\lambda = \alpha^2(L + \kappa) - L \tag{4.50}$$

where the constant α defines the spread of the sigma points around the current state vector, κ is a secondary scaling parameter usually set to zero. For parameter estimation, L is the dimension of the parameter vector θ, which reduces the number of required sigma points when compared with state estimation [89].

The augmented state vector is updated with the parameters from the previous time step, given by

$$\chi_k^f = \chi_{k-1}^a \tag{4.51}$$

The forecasted model error covariance matrix,$\mathbf{P}_k^f$, is updated using

$$\mathbf{P}_k^f = \mathbf{P}_{k-1}^a + \mathbf{Q}_{k-1} \tag{4.52}$$

where $\mathbf{Q}_{k-1}$ is the parameter error covariance at the previous time step.

A number of $2L + 1$ sigma points is defined as

$$\begin{aligned}
\chi_k^{\sigma(0)} &= \chi_k^f && (4.53)\\
\chi_k^{\sigma(j)} &= \chi_k^f + \left(\sqrt{(L+\lambda)\,\mathbf{P}_k^f}\right)_j, j = 1, \ldots, L, && (4.54)\\
\chi_k^{\sigma(j)} &= \chi_k^f - \left(\sqrt{(L+\lambda)\,\mathbf{P}_k^f}\right)_j, j = L+1, \ldots, 2L, && (4.55)
\end{aligned}$$

where $\left(\sqrt{(L+\lambda)\,\mathbf{P}_k^f}\right)_j$ is column j of the matrix square root of $(L+\lambda)\,\mathbf{P}_k^f$. Only the parameter vector is spanned out by the sigma points.

Each sigma point is used for calculating a forecast of the augmented state vector $\chi_k^{f(j)}$ using the nonlinear function $f[\cdot]$, giving

$$\begin{aligned}
\chi_k^{f(0)} &= f[\chi_k^{\sigma(0)}]\\
\chi_k^{f(1)} &= f[\chi_k^{\sigma(1)}]\\
\vdots \quad &\vdots \quad \vdots\\
\chi_k^{f(2L)} &= f[\chi_k^{\sigma(2L)}]
\end{aligned} \tag{4.56}$$

Each forecast of the augmented state vector is used for calculating a forecast of the measurement vector $\mathbf{y}_k^{f(j)}$ using the nonlinear function $h[\cdot]$, giving

$$\begin{array}{ccc} \mathbf{y}_k^{f(0)} & = & h[\chi_k^{f(0)}] \\ \mathbf{y}_k^{f(1)} & = & h[\chi_k^{f(1)}] \\ \vdots & \vdots & \vdots \\ \mathbf{y}_k^{f(2L)} & = & h[\chi_k^{f(2L)}] \end{array} \tag{4.57}$$

A weighted mean,$\overline{\mathbf{y}_k^f}$ for the forecasted measurement vectors is calculated using

$$\overline{\mathbf{y}_k^f} = \sum_{j=0}^{2L} W_m^{(j)} \mathbf{y}_k^{f(j)}, \tag{4.58}$$

$$W_m^{(0)} = \frac{\lambda}{L+\lambda}, \tag{4.59}$$

$$W_m^{(j)} = \frac{1}{2\,(L+\lambda)}, \quad j = 1, \ldots, 2L, \tag{4.60}$$

where $W_m^{(j)}$ is a weighting matrix for the mean calculation. The weight for the centre sigma points is twice the weight for the surrounding sigma points.

A weighted covariance,$\overline{\mathbf{y}_k^f}$ for the forecasted measurement vectors is calculated using

$$\mathbf{P}_k^{f,yy} = \sum_{j=0}^{2L} W_c^{(j)} \left(\mathbf{y}_k^{f(j)} - \overline{\mathbf{y}_k^f}\right) \left(\mathbf{y}_k^{f(j)} - \overline{\mathbf{y}_k^f}\right)^T + \mathbf{R}_k, \tag{4.61}$$

$$\mathbf{P}_k^{f,xy} = \sum_{j=0}^{2L} W_c^{(j)} \left(\chi_k^{\sigma(j)} - \chi_k^f\right) \left(\mathbf{y}_k^{f(j)} - \overline{\mathbf{y}_k^f}\right)^T, \tag{4.62}$$

$$W_c^{(0)} = \frac{\lambda}{L+\lambda} + (1 - \alpha^2 + \beta), \tag{4.63}$$

$$W_c^{(j)} = \frac{1}{2\,(L+\lambda)}, \quad j = 1, \ldots, 2L, \tag{4.64}$$

where $W_c^{(j)}$ is a weighting matrix for the covariance. The scaling parameter β is used to include information about the distribution. For Gaussian distribution, $\beta = 2$.

The Kalman gain, $\mathbf{K}_k$ and the analyzed parameter update χ_k^a, and the analyzed parameter error covariance update $\mathbf{P}_k^a$ is given by

$$\mathbf{K}_k = \mathbf{P}_k^{f,xy} (\mathbf{P}_k^{f,yy})^{-1} \tag{4.65}$$

$$\chi_k^a = \chi_k^f + \mathbf{K}_k \left(\mathbf{y}_k^m - \overline{\mathbf{y}_k^f} \right) \tag{4.66}$$

$$\mathbf{P}_k^a = \mathbf{P}_k^f - \mathbf{K}_k \mathbf{P}_k^{f,yy} {\mathbf{K}_k}^T \tag{4.67}$$

The UKF has shown to give smaller error estimate than the EKF [89]. In the current work, the unscented Kalman filter has been used for estimating reservoir parameters during drilling operations combined with a model predictive control algorithm for adjusting the choke valve [61, 62].

Case-based comparison of the described Kalman filters

In this section a brief example is given to compare the results from various Kalman filter methods described above. The case used is an UBD case where a 2000 m deep well is extended into a reservoir with a production index of 0.04 kg/s/bar and reservoir pressure of 230 bar. The goal is to estimate the reservoir production index using measurements of flow rates and pressures. Initially, the reservoir production index is assumed to be 0.06 kg/s/bar. The measurements have been synthetically generated using the low-order well model with 7 states, described in Section 4.2.1, adding normal distributed noise with zero mean and a standard deviation of 1% to the simulation results.

Fig. 4.7 shows the penetration rate into the reservoir and the resulting well depth. The drilling rate is 0.01 m/s and the well depth is inceased from 2000 m to 2023 m after 85 minutes including drilling breaks due to pipe connections.

The drilling fluid is a two-phase fluid consisting of liquid and gas. This results in a compressible driling fluid. Fig. 4.8 presents the drilling fluid rates at various positions of the well. The flow rate out of the well is nearly steady state when the drilling is initiated after 18 minutes. After 24 minutes a pipe connection is needed, and the circulation pumps are stopped for 10 minutes. A new pipe connection is performed after 66 minutes. Since the drilling fluid is compressible, the drilling fluid continues to flow out of the well. In addition the annulus BHP is reduced, leading to an increased flow rate from the reservoir.

The resulting annulus pressure at the bottom of the well is shown in Fig. 4.9, in addition to the choke valve differential pressure. The pressure is reduced when the drillstring fluid pumps are stopped, due to reduced friction pressure loss.

To compare the three different Kalman filters, the reservoir production index during the UBD operation is estimated using each of the filters. Regarding the computational load, the EKF requires a linearization of the state model , $f[\cdot]$, and the measurement model,$h[\cdot]$, at each time step. The dimension of the state is 7 and gives an indication of the computational load. For

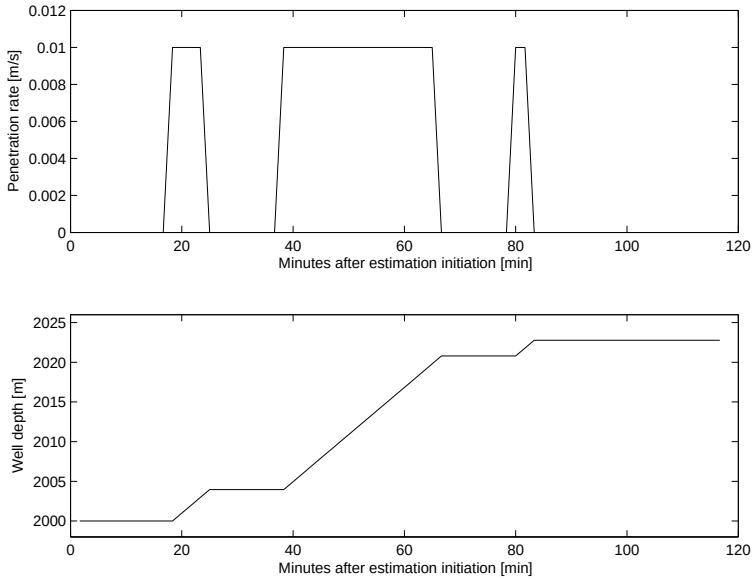

Figure 4.7: The top diagram shows the penetration rate of the drillstring, and the bottom diagram shows the depth of the well.

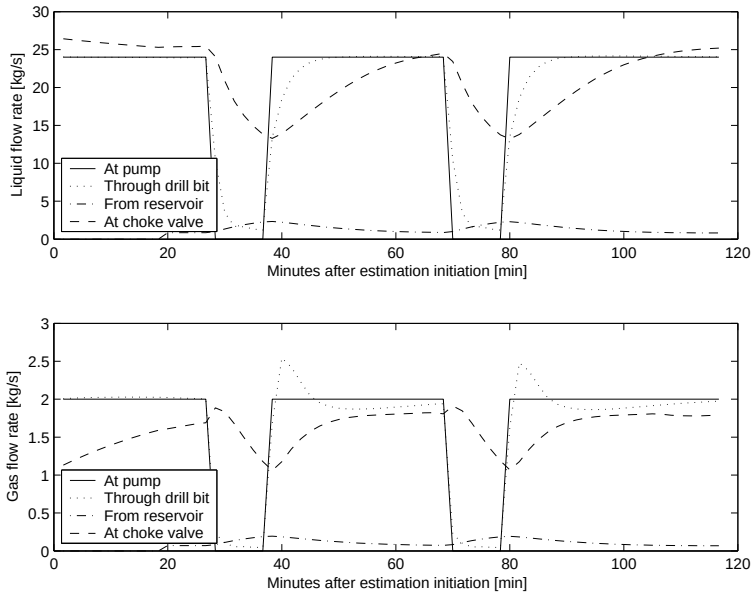

Figure 4.8: The top diagram shows the liquid flow rates in the well. The bottom diagram shows the gas flow rates in the well.

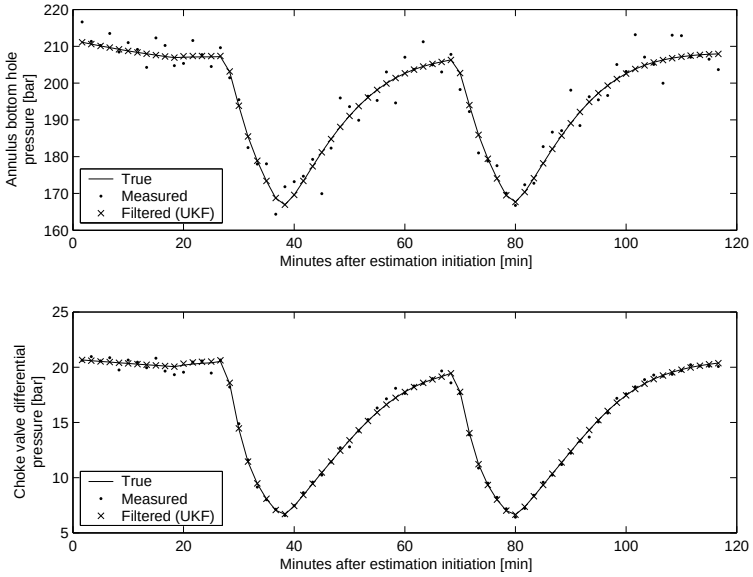

Figure 4.9: The top diagram shows the annulus BHP in the well. The bottom diagram shows the differential pressure across the choke valve.

the EnKF filter, the computation load is 100 times one model calculation time step, since a number of 100 ensemble members have been used in the analysis. However, the number of ensemble member can be reduced, and this will reduce the computational load of the EnKF. The UKF filter only requires a computational load of 3 times one model calculation time step since only a single parameter is estimated.

The results from the estimation process are shown in Fig. 4.10. All filters are started with an initial reservoir production index parameter guess of 0.06 kg/s/bar, and the true parameter is 0.04 kg/s/bar. The results show that all three Kalman filters are able to estimate the parameters quite well, both during the circulation periods, the drilling periods and the pipe connections.

In Fig. 4.11, the squared deviation from the true parameter are shown. The range of the plot has been reduced, showing the deviation from the true value during the stable region of the estimates from 25 minutes to 120 minutes. The plot shows that the UKF gives the best estimate, and that the EKF gives the estimate that deviates most from the true value.

In Fig. 4.12, the sums of the squared deviation from the true parameter when using the various Kalman filters, are shown as bar graphs, both the total sum from 18 minutes to 120 minutes and the partial sum where the estimates are nearly stable. The partial sum is calculated based on the estimates from from 25 minutes to 120 minutes. Both bar graphs show that the UKF gives

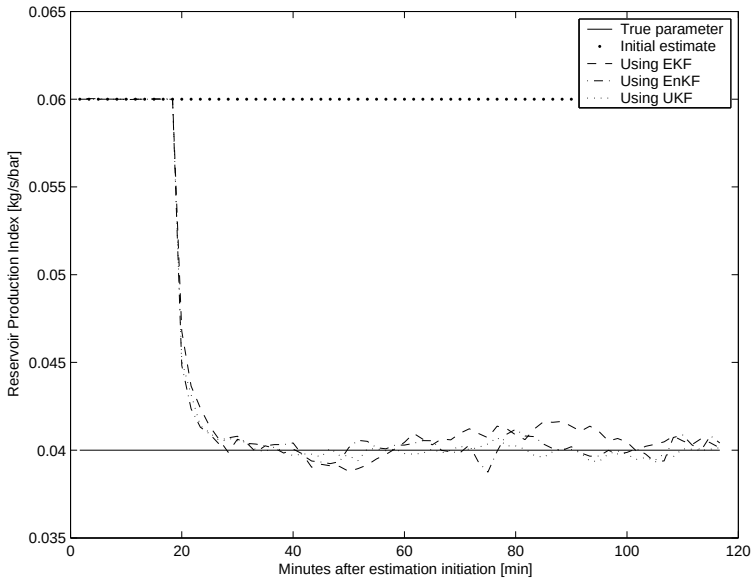

Figure 4.10: The diagram shows how the various Kalman filters converge to the correct parameter for the reservoir production index used in the model.

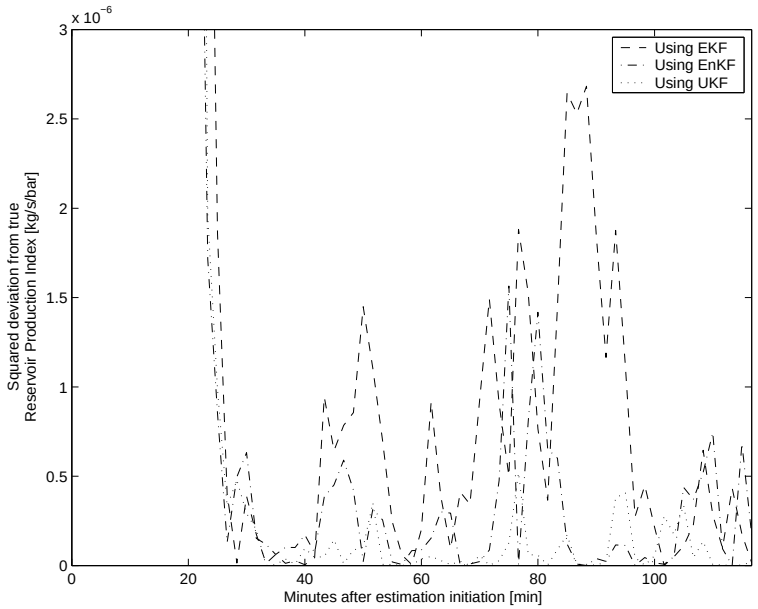

Figure 4.11: The diagram shows the calculated squared difference between the true reservoir production index parameter and the estimated parameter using the various Kalman filters.

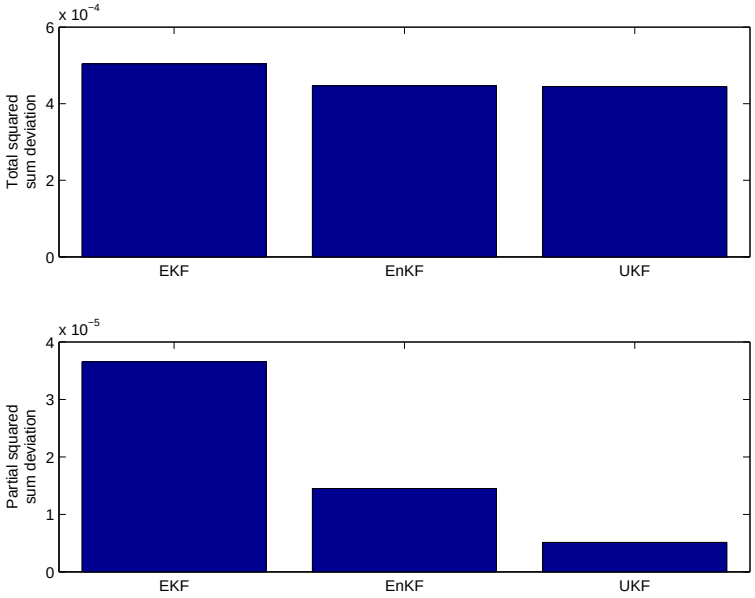

Figure 4.12: The upper bar graph shows the least squared sum of the difference between true and estimated reservoir parameters during the whole estimation period from 18 to 120 minutes. The lower diagram shows the least squared sum of the difference between true and estimated reservoir parameters during the stabilized period from 25 minutes to 120 minutes.

the best estimate, and that the EKF gives the estimate that deviates most from the true value. The comparison of the three filters is based on this single case only, and gives only an indication of the perfomance of the filters. Based on the performance of the filters and the discussion of the computational load of the filters, the UKF filter might be a good selection for further analysis.

Chapter 5

Multi Sensor Data Fusion - Examples

This chapter presents three examples where MSDF is used for estimating various parameters that are difficult to measure directly. The first example has been carried out during an early phase of the research project, and the two last examples have been carried out during the last part of the research project.

In the first example, the flow rates from pipe junctions are estimated using sensor data from several temperature probes in a laboratory test rig. The laboratory test rig is designed for emulating fluid flow during UBD.

The second example is a synthetic case where the fluid friction parameter and the gas slip parameters are estimated during the unloading phase of a UBD operation, prior to drilling into the reservoir. The reservoir pore pressure parameter is estimated during the drilling phase. Various instrumentation layouts are tested and analysed focusing on different locations of pressure sensors and flow sensors. Currently available sensors, in addition to future sensors are used in the evaluations.

In the third example, sensor data from a full scale experiment at a test site in Taquipe, Brazil is used for estimating the friction parameters and gas slip parameters of the fluid flow. No drilling is performed in this case. The test well is instrumented with pressure sensors currently not available in real applications.

5.1 Estimating pipe junction influx using temperature sensor array

In this section a soft-sensor method is presented that can be used for measuring the fluid flow rate from the reservoir to the well. First, the selection of sensors is discussed. Then a model is presented, describing the temperature and fluid flow behaviour of the experiment. A description of the experimental rig setup is given, and finally the results are presented and discussed.

5.1.1 Sensor selection

The motivation for this example is that measurements of the temperature gradient along the annulus will contain information about the amount of reservoir fluids flowing into the annulus. Since this type of measurement is not currently taken during UBD, there are no real data currently available. A test rig simulating the actual process has been designed and constructed. The focus has been on measuring the temperature in the annulus which varies due to mixing and transportation of the fluids. Currently no temperature sensor array is commercially available for measuring the actual fluid temperature in the well annulus. One type of sensor array that currently is the best candidate for such an application, is the fibre optic temperature sensor. Currently, the sensor array is used for temperature sensing in production wells. The data can be used for giving a production flow estimate [38]. In the experimental test rig, standard Pt100 elements are chosen for convenience. The main purpose of the experiment is to evaluate methods for analysing the data from the temperature array. Different methods for extracting the inflow data are used and evaluated, using steady state temperature data.

5.1.2 Modelling thermal properties in fluid flow

An important part when analysing the temperature data given from the sensors, is to have a good physical understanding of the heat transfer during the mixing of fluids and the fluid flow. A steady state temperature modelling approach is used for modelling the temperature difference along the pipe.

Based upon the flow data, the temperature profile can be calculated using the thermodynamic models. The added heat to the system is given by

$$Q = mc_p\Delta T, \tag{5.1}$$

where Q is the added energy, m is the mass, c_p is the specific heat capacity and ΔT is the temperature increase.

Table 5.1: Actual flow rates in oil well

Flow type	**Volume flow rates [l/min]**
Circulating flow	1920
Inflow from Zone 1	180
Inflow from Zone 2	96
Inflow from Zone 3	480

Since water is used both as the injected fluid and the original fluid, and mass is proportional to mass flow rate, the resulting temperature due to injection of warm water is

$$T_r = \frac{q_o T_o + q_i T_i}{q_o + q_i} \tag{5.2}$$

where T_r is the resulting temperature, T_o is the original temperature T_i is the injected temperature, q_o the original flow, and q_i is the injected flow. If we in addition assume that there are negligible losses to the environment, then the resulting temperature can be calculated.

5.1.3 Description of the experimental test rig

The test rig is scaled to fit the 20 m long laboratory. The main scaling restriction is to make sure that the fluid uses the same time to flow through the pipe section as it uses to flow through the well. The methodology for scaling the experiment is to scale the length of the reservoir section to the corresponding pipe section. The inner diameter of the pipe is scaled accordingly. The fluid velocity in the pipe is scaled to keep the same transportation delay as in the well. In [85], a 2000 m deep well with three 300 m long reservoir zones is simulated and the flow rates are calculated. The flow rates are presented in Table 5.1.

The length of each reservoir zone is 100 m and the hydraulic diameter is 0.1822 m. To scale down the experiment to fit the laboratory, an experiment pipe length of 18 m is selected. The pipe inner diameter is selected to be 0.027 m. The fluid velocity in the well is 1.226 m/s, and hence the equivalent fluid velocity in the pipe should be 0.0735 m/s. This results in the equivalent flow rates inside the pipe as given in Table 5.2.

The reservoir fluid migrates into the well along the reservoir section of the well, but for simplicity a point inflow configuration is simulated for the experiment test rig case. The temperatures at the inflow points are equal to

Table 5.2: Equivalent flow rates in experimental test rig

Flow type	**Volume flow rates [l/min]**
Circulating flow	2.6
Inflow from Zone 1	0.24
Inflow from Zone 2	0.13
Inflow from Zone 3	0.63

each other. The temperature difference between the reservoir fluids and the circulation fluids is around 20 °C.

The experiment test rig consistes of three 6 m long pipe segments. Between each pipe segment a T-fitting is mounted, and 3 pipes are connected to supply warm fluid into the pipe. Temperature is measured at each inflow, and also at the main cold fluid inflow at the end of the pipe. As test fluid, water is selected for convenience. The rig is equivalent to the annulus part of the oil well. The cold water is flowing into the main pipe in one end, which is equivalent to the drill bit. As the fluid is flowing towards the outlet, it is mixed with the warm fluid, which is injected at the three junctions along the pipe.

Six temperature sensors are placed with 1 m distance along each pipe segments, leading to 18 sensors along the main pipe. In addition, the temperatures at each inflow are also measured, leading to a total of 22 temperature sensors. The temperature sensors are logged using NI LabView FieldPoint Pt100 temperature modules, which are connected to a PC [56].

Flow sensors are mounted at each inflow and at the outflow. Measurements of the main inflow and the main outflow are typically available in a real application, and the three flow meters at the warm fluid inflow points are used as reference sensors. A piping and instrument diagram is shown in Fig. 5.1. The flow meters are connected to a NI LabView frequency data acquisition cards.

5.1.4 Measurements and discussion

Measurements are carried out to test and evaluate the various flow estimation methods. A total of 47 temperature profiles are logged, and these are performed during 3 different series. The main inflow temperature (9 °C) is the same in all the series. Series 1 uses a warm inflow temperature at 26 °C and 12 different inflow profiles are logged. Series 2 uses a warm inflow temperature at 24 °C and 20 different inflow profiles are logged. Series 3 uses a

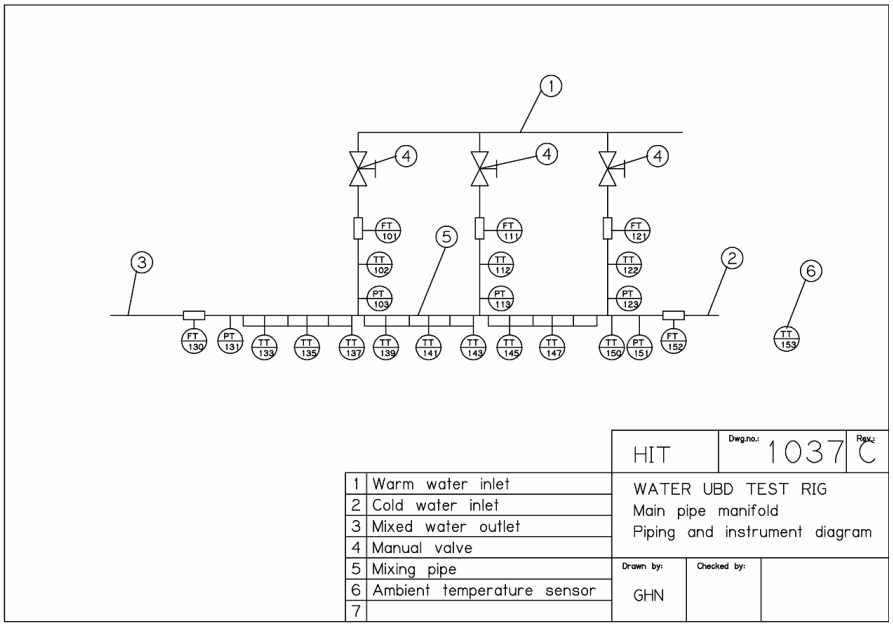

Figure 5.1: Piping and instrumentation diagram for the experimental test rig.

warm inflow temperature at 32 °C and 15 different inflow profiles are logged.

Some of the profiles which are logged, have one or more of the warm inflow valves closed. Only the flow profiles where all the valves are open, are included in this analysis. Estimations of inflow rates using the Levenberq-Marquardt algorithm are carried out for each flow profile. The uncertainties in the measurements which are used for estimation, are given as one standard deviation, and are set to 0.72 l/min, 0.2 bar and 0.1 °C. Similar results are found for each series, so only the results in series 3 are presented.

In the third series, 9 profiles are logged where all the valves were open. The measured and estimated data are presented in Fig. 5.2. The data for each profile are grouped together, showing measured and estimated data for each inflow pipe.

From the warm inflow estimates we find that there is fairly good agreement between the measured flow and the estimated flow. However, for measured flow values above 2 l/min, the estimated values tend to underestimate the flow. Regarding the temperature values there seems to be a good match between the values. The Levenberg-Marquardt estimation algorithm manages to estimate the inflow fairly well. The uncertainty in the estimation algorithm lies in the values of the flow sensor readings.

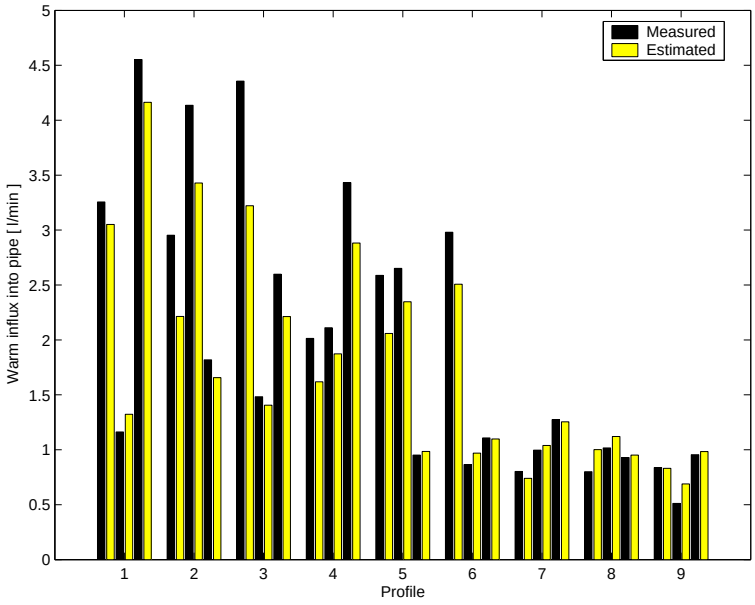

Figure 5.2: Measured and estimated warm inflow for 9 profiles in Series 3.

Table 5.3: Neural net layer topology

Layer	**Layer width**	**Function type**
Input	22	
1st	35	`'logsig'`
2nd	20	`'logsig'`
3rd	10	`'logsig'`
Output	3	`'purelin'`

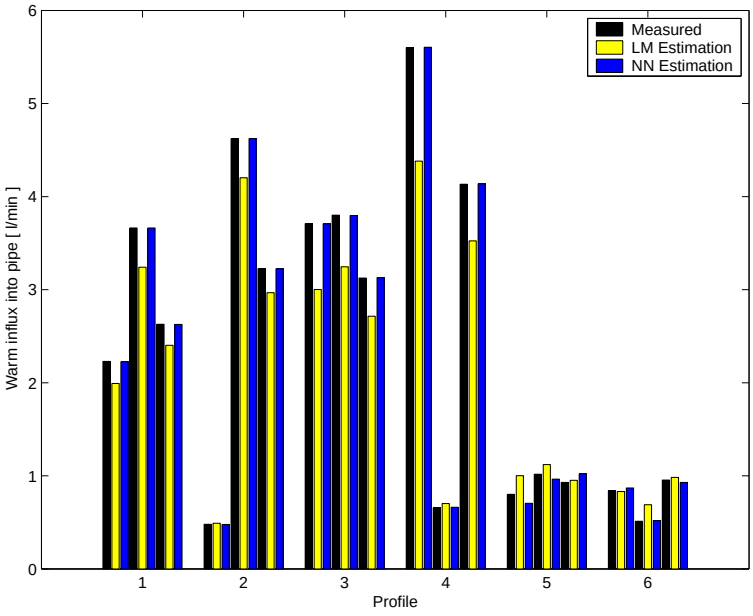

Figure 5.3: Comparison between measured data, Levenberg-Marquardt estimations and Neural Net estimations.

A neural net is trained with the available data sets to estimate the inflow rate. Table 5.3 gives an overview of the neural network layer topology. The function type `'logsig'` is the log-sigmoid neural transfer function, and the function type `'purelin'` is the linear neural transfer function [21]. Based on the main inflow and outflow measurements, the temperature profile along the pipe and the warm inflow temperature is used to estimate the in-flow rate profile. All the available measured inflow profiles is used to train the network. The measured and estimated data were compared with the estimation results from using the Levenberg-Marquardt algorithm.

The last two profiles in each series is shown in Fig. 5.3, and the results indicates that the neural net estimates are nearly equal to the measured values. This is as expected, since the neural net acts a multivariable function approximation for the inverse flow function, where the temperature and main flow values are used to calculate the warm inflow profile.

Regarding the Levenberg-Marquardt estimations, these estimations are based upon the mathematical model of the test rig. As mentioned, there are some differences between the modelled data and the measured data. These differences between the model data and the measured data can lead to differences in the Levenberg-Marquardt estimation results.

Table 5.4: Constant parameters used in example

Model parameters	Value
Compressibility of injection liquid	1.0e-9 Pa^{-1}
Compressibility of production liquid	1.17e-9 Pa^{-1}
Viscosity of injection liquid	0.001 Pa.s
Viscosity of production liquid	0.04 Pa.s
Wellbore radius	0.075 m
Penetration rate in the formation	0.01 m/s
Uncertainty in pressure measurements. (standard deviation)	0.1 bar
Uncertainty in flow rate measurements. (standard deviation)	0.1 %

5.2 Estimating fluid flow and reservoir parameters using pressure sensor arrays and non-intrusive sensors

When estimating reservior parameters based upon pressure and flow measurements in the well annulus, it is important that the model used for parameter estimation describes the physical behaviour of the flow. If some of the well fluid flow parameters are uncertain such as the friction parameter f and the gas slip relation parameters, K and S, then these parameters should be estimated before reservoir parameters are estimated, such as the reservoir pressure p_{res}. This example shows the use of the ensemble Kalman filter to estimate both annulus fluid flow parameters and the reservoir parameters in a simulated test case [57].

5.2.1 Description of the well and reservoir

The well consists of a casing with an inner diameter of 0.18 m, and a drillstring with an inner diameter of 0.075 m. The well length is 1262 m. A parasite string for nitrogen injection with an inner diameter of 0.05 m is connected to the casing at 760 m depth. Some of the reservoir parameters are known, including the reservoir permeability at 350 mD and the reservoir porosity at 0.18. Other constant parameters are given in Table 5.4, and the values are typical for a real well.

For modelling the fluid flow in the well and the reservoir, the detailed model described in Section 4.2.2 is used. The slip relation between the gas

Table 5.5: Estimation of parameters

Parameter	**Initial value**	**True value**
f (friction)	0.010	0.012
K (slip gradient)	1.2	1.1
S (slip zero point)	0.55	0.40
p_{res} (reservoir pressure)	120 bar	110 bar

and the liquid is calculated using a linear relation between the velocity of the gas and velocity of the mixture, given by

$$v_g = Kv_{mix} + S. \tag{5.3}$$

The friction pressure loss is modelled using a constant friction parameter f. The inflow from the reservoir is modelled using Eq. (3.11). To match the combined well-reservoir model with the measured data, the model parameters f, K, S and p_{res} are estimated. The initial and true values of the parameters chosen for estimation are given in Table 5.5. The true values are used for generating the syntetically mmeasurements, and the initial values are the "best guess" prior to the drilling operation.

Initially the well is circulated using water at a rate of 600 l/min. After 7 minutes, nitrogen gas at standard conditions are injected into the annulus at a rate of 8500 l/min using the parasite string. The well is unloaded, and stable pressure conditions are present after 60 minutes. The drilling initiates after 67 minutes, and lasts until 117 minutes. Afterwards, the well is only circulated and no further drilling is performed.

The BHPs are presented in Fig. 5.4, where both the simulation using the true parameters and the simulation using the initial parameters are given. The uncalibrated parameters are resulting in an over-estimation of the pressures in the well of about 3 bar.

The reservoir inflow measured at the wellhead are given in Fig. 5.5. Since the un-calibrated simulation assumes a reservoir pressure of about 10 bar higher than the true value, the un-calibrated inflow is nearly the double of the true inflow.

5.2.2 Sensor selection

The ensemble Kalman filter is tested using three different instrumentation layouts. The first layout is a standard drilling setup, using a single bottom-hole sensor and a fluid flow meter at the wellhead. The second layout is also

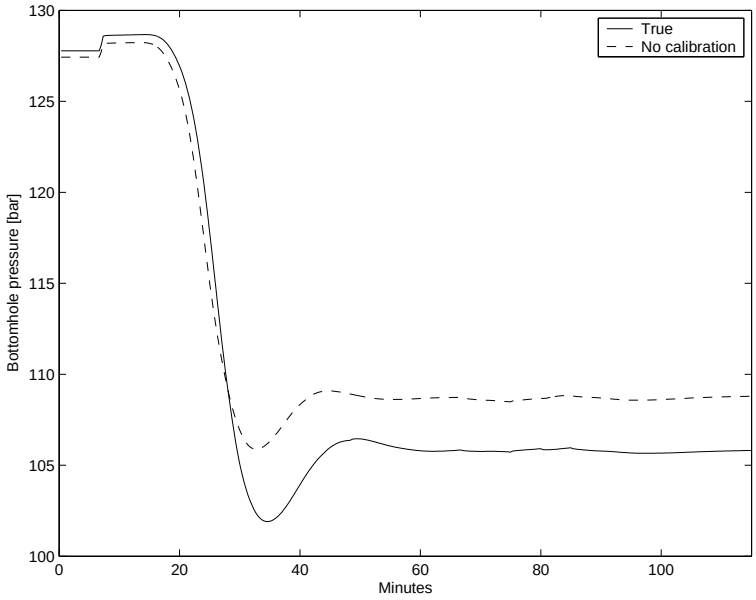

Figure 5.4: Comparison of BHP using true and un-calibrated model parameters.

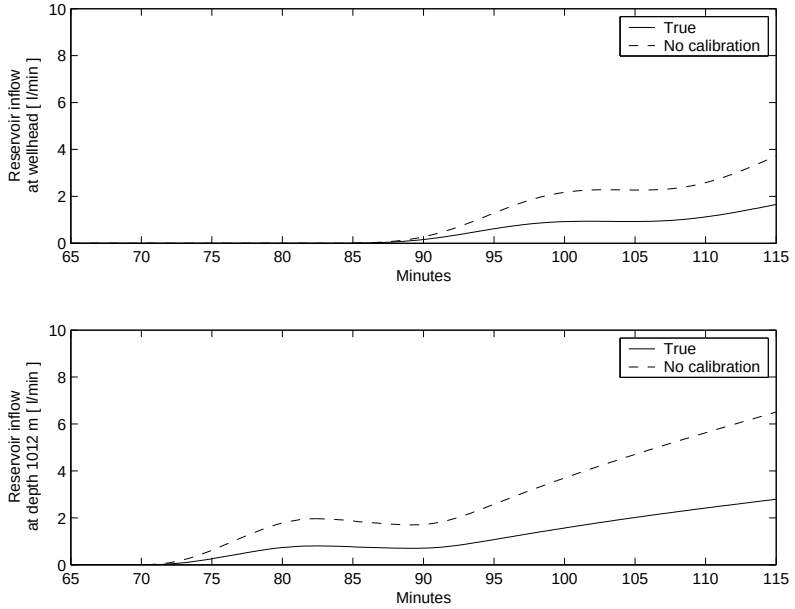

Figure 5.5: Comparison of inflow rate measured at wellhead (top) and casing shoe (bottom) using true and uncalibrated fluid flow and reservoir parameters.

using a fluid flow meter at the top, but in addition an array of 19 pressure sensors are placed along the drillstring, measuring the pressure at various positions in the annulus ranging from the bottomhole assembly to 200 m above the bottomhole assembly. The data from the sensors can be transmitted using a cable which is incorporated into the drillstring as discussed in Section 4.1.2. The third layout uses the same array of pressure sensors, but in addition to measuring the flow at the wellhead, the flow is measured at the casing shoe depth of 1012 m. A design concept for such a non-intrusive annulus flowmeter is described in Section 4.1.4.

5.2.3 Results and discussions

The estimation of the parameters is improved as more instruments are added. Fig. 5.6 shows the estimation and the calculated uncertainty of the fluid flow friction parameter, f. Using only the single bottomhole sensor, the estimated parameter fluctuates around the true value the first 40 minutes of the case, but manages to converge to the correct value after 50 minutes. The parameter estimation is improving a lot when using the downhole pressure sensor array. When the downhole flow sensor is added, the estimates are converging quite fast. The main difference between the uncertainties of the friction parameter estimates is between when using the single downhole pressure sensor and the array of downhole pressure sensors.

When looking at the gradient parameter for the gas-slip, K, shown in Fig. 5.7 and the zeropoint parameter for the gas slip, S, shown in Fig. 5.8, there is very little difference between the estimates using the various instrumentation layouts, both regarding the estimated values and the uncertainties of the estimates. The parameters converge to the true values within the first 40 minutes, and the uncertainties are reduced accordingly.

The main difference between the instrumentation layouts is seen when calibrating the reservoir pore pressure, p_{res}. When using the single downhole sensor, the estimate shows only a tendency to converge to the true value when the drilling is stopped at 117 minutes, as seen in Fig 5.9. The uncertainty of the pore pressure estimate is about 3 bar. When introducing the pressure sensor array, the estimate converges to the true value with an uncertainty below 1.5 bar. Finally, adding the downhole flow sensor, the reservoir pore pressure estimate converges fast to the true value, with an uncertainty below 1 bar already 15 minutes after the start of drilling.

The results show that introducing pressure sensors along the drillstring, improves the characterization of the reservoir. The introduction of a downhole non-intrusive flowmeter will further reduce the uncertainty of the estimated reservoir parameters. The results also show that the ensemble Kalman

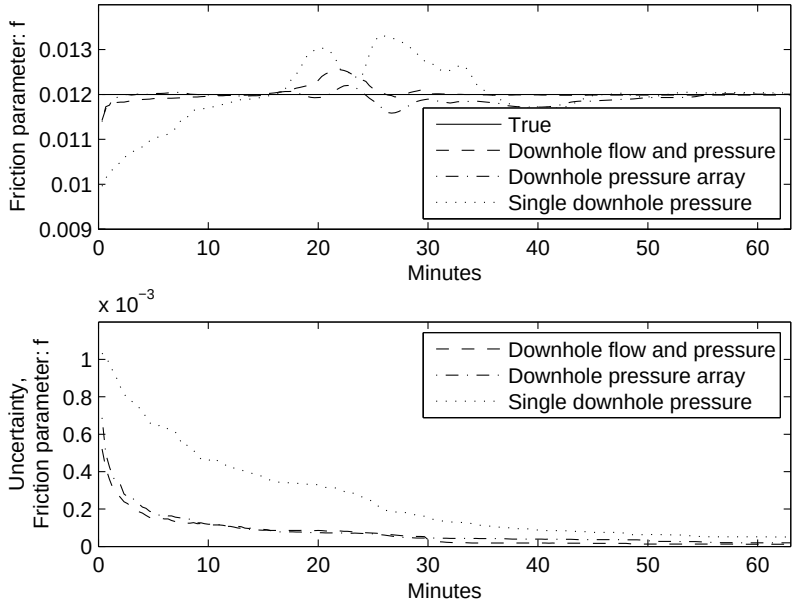

Figure 5.6: Comparing the estimates of the friction factor parameter, f, and the corresponding calculated uncertainty using various sensor layouts.

filter can be used for estimating model parameters having various instrumentation layouts.

The reservoir model in this study is rather simple, modelling a homogeneous reservoir. A more complex reservoir model allowing for fractures and other heterogeneities can be developed and included in the analysis. The possibility of extracting additional information about the reservoir based on the measurements can also be examined.

The cost of introducing the various sensors is not taken into account. A request for additional sensors will impose additional investment and maintenance. A study for selecting the best sensor layout based on both the quality of information gained from the sensors and the cost of the sensor can be preformed. For a given drilling operation this can be carried out similar to what is done for prediction of reservoir inflow in production wells [4, 55].

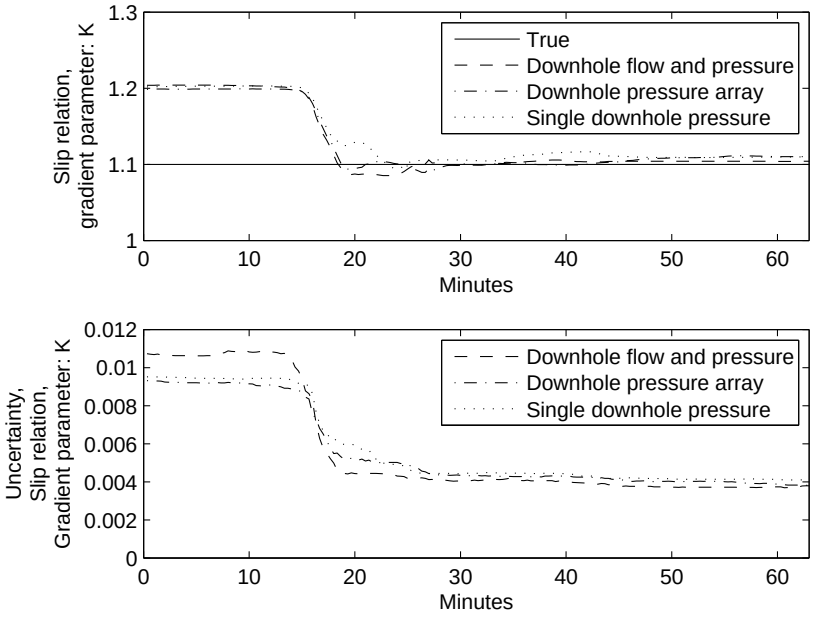

Figure 5.7: Comparing the estimates of the slip relation gradient parameter, K, and the corresponding calculated uncertainty using various sensor layouts.

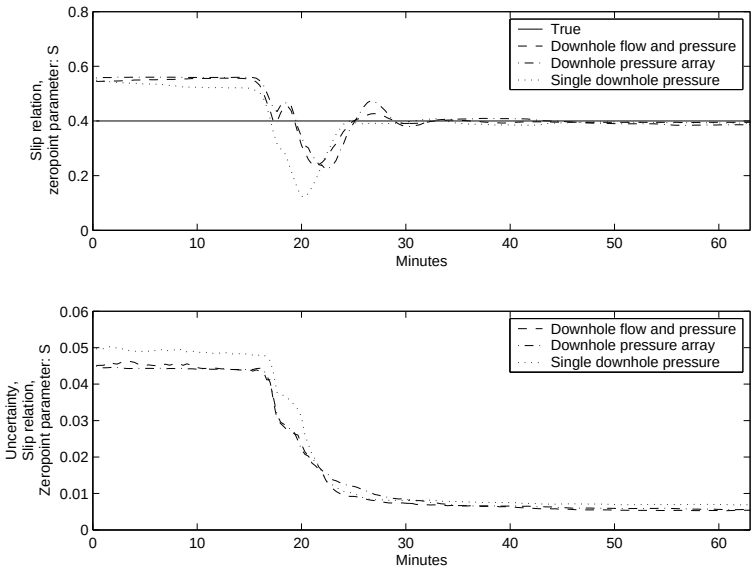

Figure 5.8: Comparing the estimates of the slip relation zeropoint parameter, S, and the corresponding calculated uncertainty using various sensor layouts.

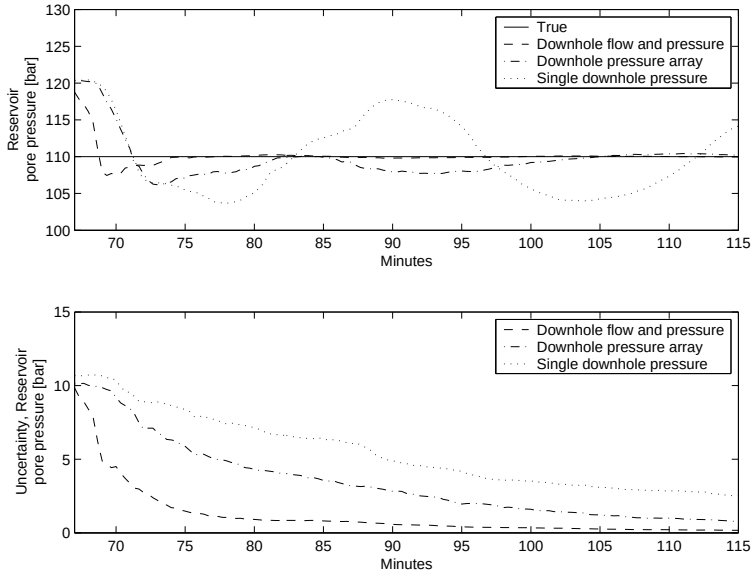

Figure 5.9: Comparing the estimates of the reservoir pore pressure, p_{res} and the corresponding calculated uncertainty using various sensor layouts.

5.3 Estimating fluid flow parameters using pressure sensor array

In the third example, full-scale experimental data from a test well in Taquipe, Brazil are used to calibrate the model. However, since no drilling is performed in this case, the model is calibrated by only estimating the fluid flow parameters, f, K and S. The idea is to show how the ensemble Kalman filter is able to estimate the fluid parameters when incorporating real measurements.

5.3.1 Description of the test well setup

Similar to the example in the previous section, the well consists of a casing with an inner diameter of 0.18 m and a drillstring with inner diameter of 0.075 m. The parasite nitrogen injection line is a tubing with inner diameter of 0.05 m that connects to the casing at the depth of 760 m. Here a check valve and an orifice are installed to control the gas flow. The wellhead choke is set to 75 % opening. Other parameters from the experiment are found in Table 5.6. During the experimental tests, different combinations of gas and liquid injection rates are used and the corresponding well pressures are logged.

The case initiates with a water-filled well where the fluid flow rate is zero.

Table 5.6: Constant parameters used in example

Model parameters	Value
Compressibility of injection liquid	1.0e-9 Pa-1
Viscosity of injection liquid	0.001 Pa.s
Wellbore radius	0.075 m
Uncertainty in pressure measurements. (standard deviation)	0.1 bar
Uncertainty in flow rate measurements. (standard deviation)	0.1 %

Then the water pump is started at a rate of 600 l/min and nitrogen gas at standard conditions is injected by a rate of 8500 l/min. The well is unloaded, and the amount of gas leads to a substantial drop in the effective BHP. The BHP is reduced to about 100 bar. This flow regime leads to challenges for well flow models, as large amount of gas are difficult to model correctly, and the predicted results often differs from real data. The steady state situation is reached after 40 minutes. The choke valve remains at the same position during the whole experiment.

5.3.2 Sensor selection

Three pressure-temperature memory sensors are attached to the drillstring at the depth of 185 m, 605 m and 998 m. In addition, the BHP is monitored by a logging tool at 1262 m depth.

In this example two different sensor layouts are used for the parameter estimation using the ensemble Kalman filter. First the estimation is performed using all the four available sensors. Secondly, the estimation is performed using only the bottomhole sensor.

5.3.3 Results and discussions

The pressure data from these parameter estimation calculations are presented in Figs. 5.10-5.13, and compared with the measurement data and data from an un-calibrated simulation. The resulting pressure data shows the best fit with measured data when using four sensors.

In Figs. 5.14-5.16 the estimated parameters are presented, and the parameters varies during the unloading period. The calculated uncertainties of the parameters are also presented. Calibration using all the four annulus pressure sensors gives the lowest uncertainty.

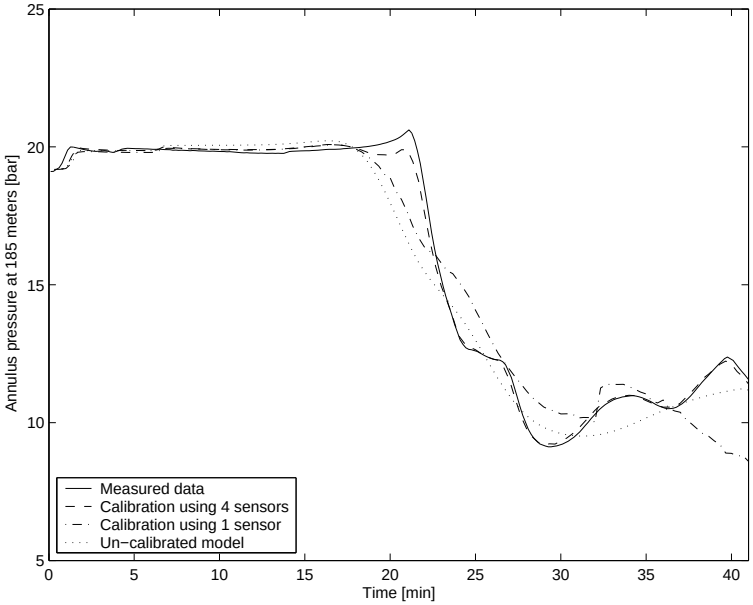

Figure 5.10: Comparing values for pressure sensor at 185 m.

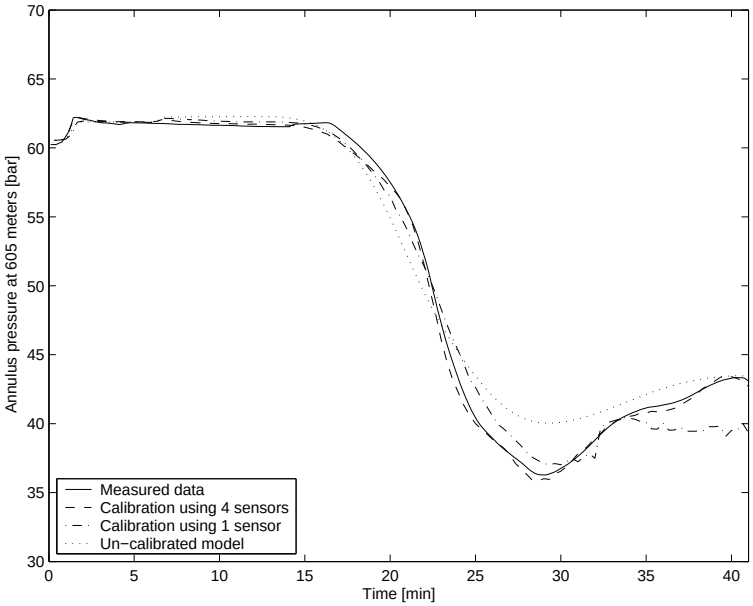

Figure 5.11: Comparing values for pressure sensor at 605 m.

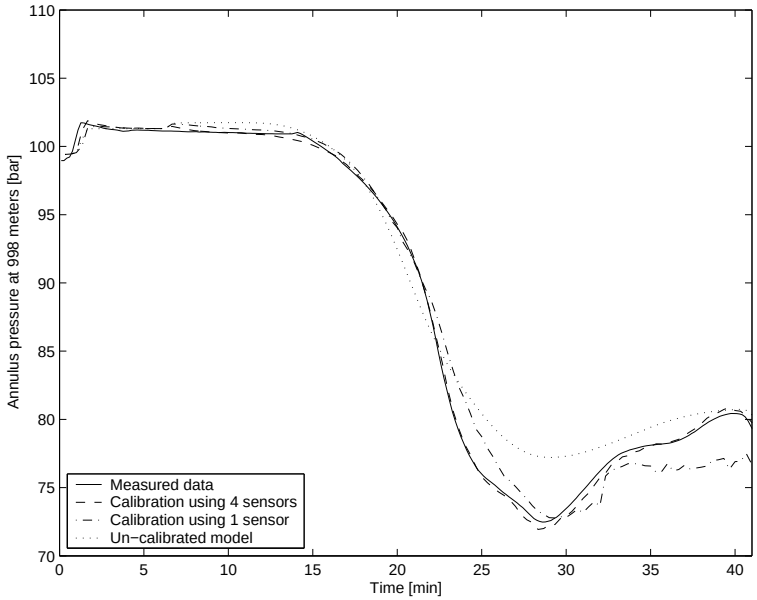

Figure 5.12: Comparing values for pressure sensor at 998 m.

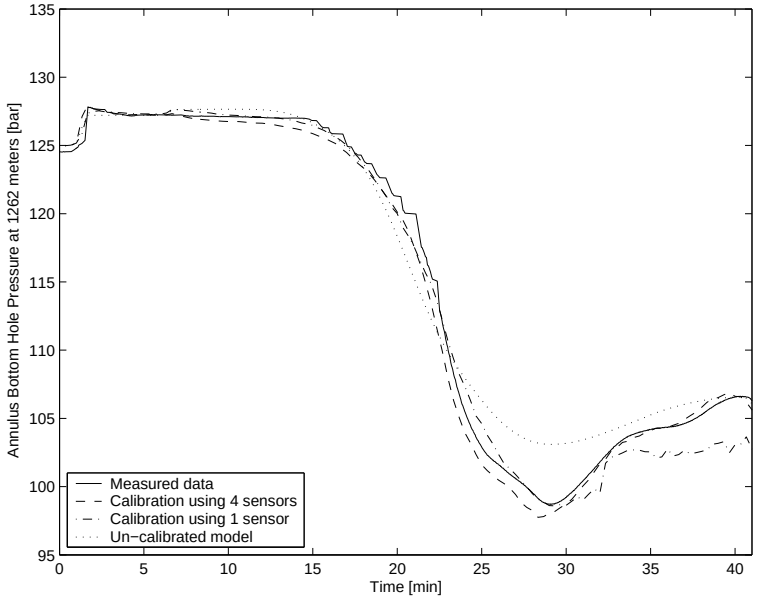

Figure 5.13: Comparing values for BHP sensor at 1262 m.

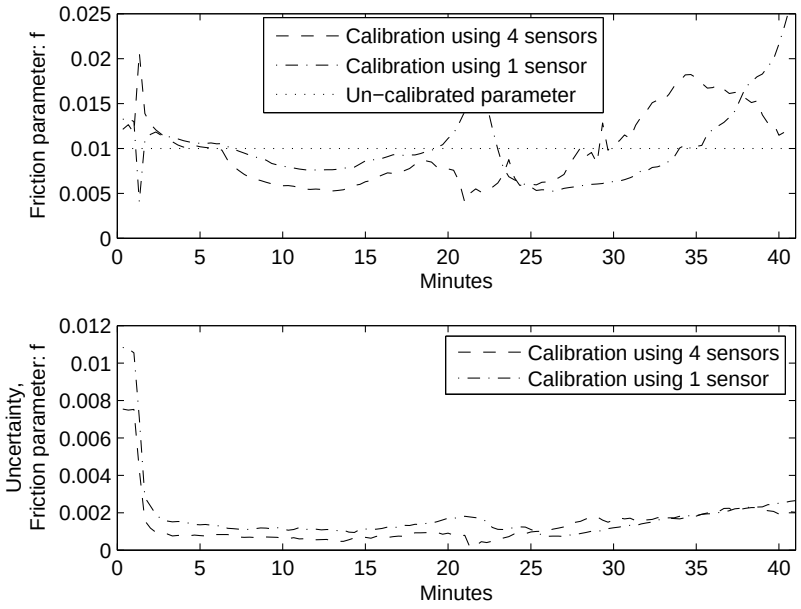

Figure 5.14: Estimates of the friction parameter f at top, and at bottom the calculated uncertainty.

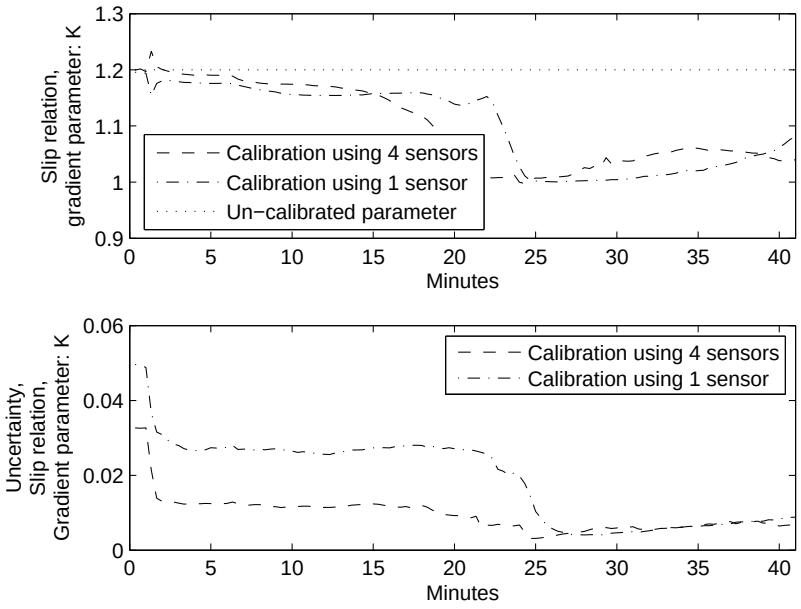

Figure 5.15: Estimates of the gas slip relation gradient parameter K at top, and at bottom the calculated uncertainty.

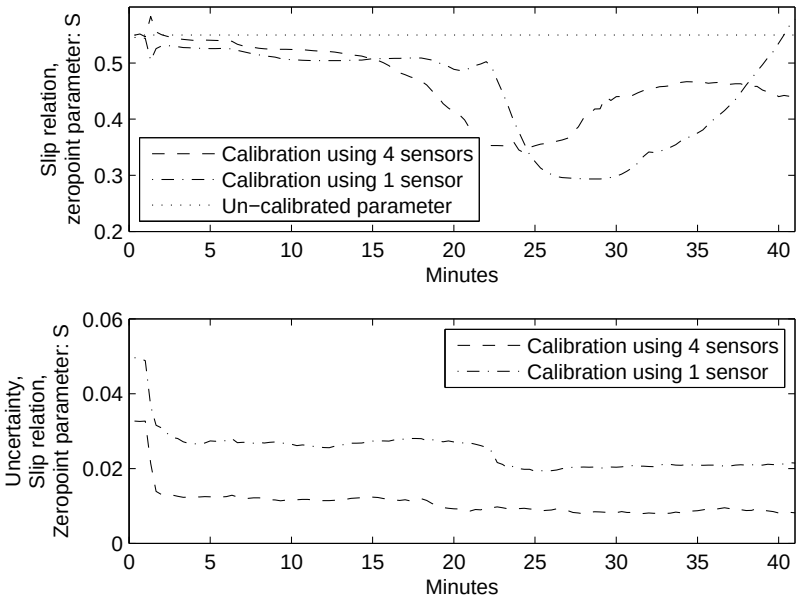

Figure 5.16: Estimates of the gas slip relation zeropoint parameter S at top, and at bottom the calculated uncertainty.

Using the ensemble Kalman filter, the measurements can be used for calibrating a real-time dynamic model of the complete drilling system. The results show that introducing more sensors along the drillstring and casing improve the estimation of the unknown model parameters.

Chapter 6

Multivariable Process Control

During UBD, there are multiple control variables that are being adjusted in order to maintain underbalanced conditions along the well section that are exposed to the reservoir. The most important control variables are drillstring fluid pump mass rate, w, drilling fluid density, ρ, and choke valve opening, z. Multiple measurements are available in order to evaluate if the underbalanced conditions are maintained. Typical measurements available are flow rates, pump pressure, choke valve differential pressure and BHP.

To contain pressure fluctuations during the drilling operations, multivariable process control is required. In [3, 77] there are descriptions of several approaches for controlling such a multivariable process. Control methods such as decoupling, feed-forward, modal control and optimal control could be used. In addition the available models of the drilling process should be utilized to improve the control system.

The three control variables, the fluid density, the fluid rate and the choke valve opening, all influence the BHP. Typically, the choke valve opening is used to control and compensate for the rapid pressure transients in the time span of a few seconds. For slower pressure variations in the time span of within a few minutes, the fluid rate is adjusted. For a longer time horizon the fluid density can be adjusted.

An important purpose of the drilling fluid is to clean the well for cuttings during the drilling process. The control of the various pump systems manipulating the fluid flow rate in the well, should be referenced to the hole cleaning efficiency. The third control variable, the fluid density, has the primary role of maintaining pressure safety barrier for avoiding uncontrolled influx of reservoir fluids. The fluid density should be kept as high as possible, but still allow for sufficient pressure margins that allows for fluid friction pressure loss both in annulus and at the choke valve opening. Fig. 6.1 describes inputs and outputs of a multivariable control system for a well.

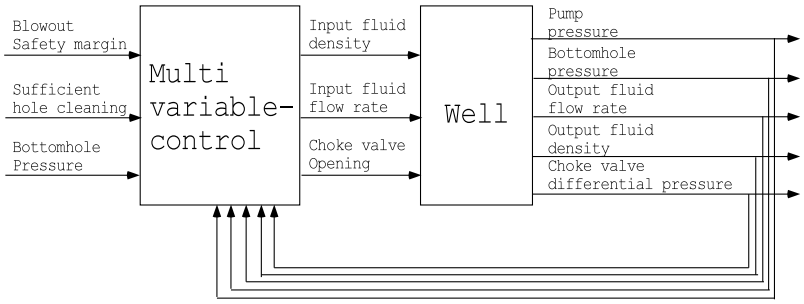

Figure 6.1: Schematic of multivariable control of a well.

In a multivariable control system for UBD operations, the three control variables is related to three different properties, the BHP, the annulus fluid flow maintaining sufficient cleaning of the hole, and the pressure safety margin. The pressure safety margin could be a percentage of the total bottomhole reference pressure. A combined automated control of all three control variables should be used during the various procedures when drilling a well, such as circulation start-up, circulation shut-down, pipe connections, hole cleaning and insertion and extraction of the drillstring.

In the present work, focus has been on two of the control variables, fluid rate and choke valve opening, keeping the third control variable, the fluid density, constant. Since the choke valve opening is able to compensate for transient pressure changes faster than the fluid rate, the focus will be on using the choke valve as the primary control variable. Two different control approaches have been used and evaluated. The first control design is using standard linear control, and the other control design is model predictive control. In this chapter a brief description of linear control and model predictive control will be given.

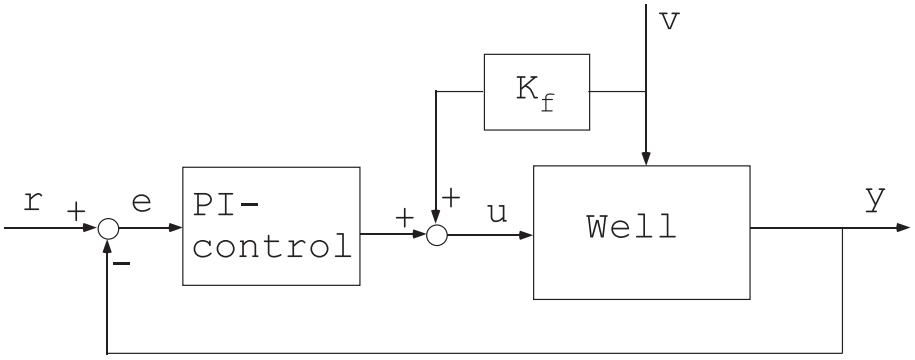

Figure 6.2: Schematic of feedback PI control including feed-forward compensation of disturbance

6.1 Linear Control

Linear control is selected to establish a basis for comparison with other control designs. For an initial evaluation, the choke valve opening is used as the primary control variable. The fluid flow rate can then be modelled as a disturbance to a single-variable control loop.

Fig. 6.2 shows a simple feedback Proportional-Integral (PI) control including feed-forward compensation of known disturbances. The PI-control method is evaluating the difference between the reference pressure value, r, and the actual pressure value in the well, y. This difference e is used as an input to the PI-control algorithm (see e.g., [79]), which relates this difference to a choke opening value. The other control variables such as the input flow rate is defined as known disturbance, v. The known disturbance is compensated for directly by changing the choke opening proportionally to the disturbance. These two effects, the feedback from the measurements and the feed-forward of the disturbance, defines an input to the choke opening set-point u. The relation between the measured parameters and the control parameter including the feed forward compensation can be described as

$$u = u_0 + K_p e + \frac{K_p}{T_i} \int_0^t e d\tau + K_f v, \tag{6.1}$$

where u_0 is the choke opening during normal drilling operations, K_p is the proportional relation between difference in pressure and choke opening, T_i is the integral time for the accumulated differences, K_f is the proportional relation between fluid flow rate and choke opening.

The PI-control method is frequently used for a variety of different process control problems. One of the main challenges when introducing such a control algorithm is to find the correct control parameters K_p, T_i and K_f. One

method for defining control parameters is to use the Ziegler-Nichols closed-loop method (see e.g., [79]), which is based on experiments where the control parameters are adjusted until the process becomes marginally stable.

Since such experiments are not possible to do during drilling, the control setting can be found by using a model of the system. If a detailed model of the actual well is not available, then a simple low-order model of the process might be developed and tuned based on measurement from a real well. In [80], a low-order dynamic model is developed for controlling slug flow in a gas-lifted production well. An equivalent model for the UBD case has been developed and the control parameters have been found based on experiments performed on the low-order model. [58].

The described linear control system using the choke control valve opening as the primary control variable can be expanded to a multivariable control system, including the fluid flow rate and the fluid density as control variables. The measurements of fluid flow rate out of the annulus and the total pressure safety margin could then be used in a decoupled control design or an optimal control design. However, since the process is highly nonlinear, defining the control parameters for the various drilling scenarios will require detailed analysis for the whole range of fluid densities, fluid flow rates and choke valve openings.

6.2 Nonlinear Model Predictive Control

Model prediction control is well suited for multivariable control design where the control variables interact closely(see e.g., [50]). Model Predictive Control uses a model to predict the future behaviour of the system. The optimal control setting is then chosen based on an optimization algorithm which minimizes the error between the reference set-point and the future predicted measurements settings.

Since the two-phase flow in the well is highly non-linear, a model describing the fluid behaviour is developed. Then a non-linear optimization algorithm is being used, resulting in a non-linear model predictive control (NMPC) method. Fig. 6.3 shows a schematic of a well system with the proposed control method, where r is the reference pressure value, y is the actual pressure value in the well, v is the known disturbances such as the flow rate into the well, and u is the choke opening set-point.

The model used for prediction is a numerical implementation of the partial differential equations of the well system, and a least-squares non-linear optimization method is used for selecting the choke opening set-points. The model is used to predict the pressures at certain time steps ahead in time.

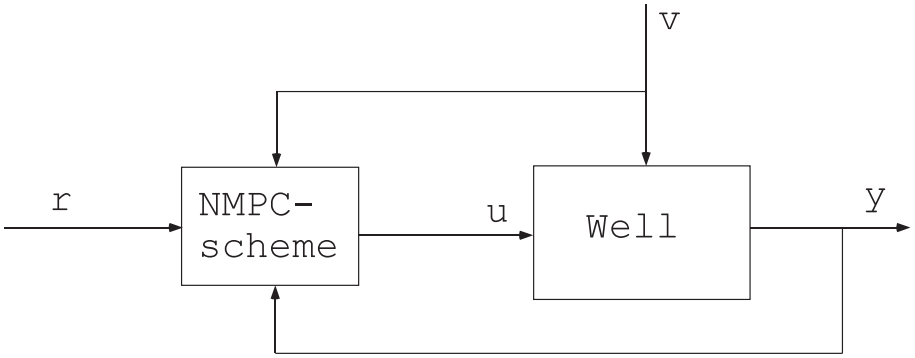

Figure 6.3: Diagram of a well system with nonlinear model predictive control algorithm.

The notation used here is similar to the notation used in [50], and $r\left(k+i|k\right)$ is used to describe a reference value r valid at the future time steps $k+i$ evaluated at the current time step k. The future time steps is denoted $k+i$, where i is the amount of time steps ahead in time, given as $i=[1,2,\ldots,H_p]$, where H_p is the prediction horizon. We chose the reference trajectory r at the time step $t=k$ as

$$r\left(k+i|k\right)=y_{ref}-\left[\left(y_{ref}-\hat{y}\left(k\right)\right)e^{\left(-iT_s/T_{ref}\right)}\right],i=1,2,\ldots,H_p \tag{6.2}$$

where y_{ref} is the reference pressure, $\hat{y}\left(k\right)$ is the modelled pressure at the current time step, T_s is the time step duration, and T_{ref} is the time response. The state model f_P and sensor model g_P is used to predict the future pressures of the well, and the input $\hat{u}\left(k+i|k\right)$ is applied over the horizon $i=[1,2,\ldots,H_p]$,

$$\begin{aligned}\hat{x}\left(k+i|k\right) &= f_P\left[\hat{x}\left(k+i-1|k\right),\hat{u}\left(k+i|k\right),\ldots,\hat{u}\left(k|k\right)\right] &(6.3)\\ \hat{y}\left(k+i|k\right) &= g_P\left[\hat{x}\left(k+i|k\right)\right], &(6.4)\end{aligned}$$

where f_P and g_P is calculated using the detailed model using spatial discretization. To find the optimal input trajectory, $\hat{u}_{opt}\left(k-i|k\right)$, a least square cost criterion is defined by

$$S\left(r,\hat{y}\right)=\sum_{i\in P}\left[r\left(k+i|k\right)-\hat{y}\left(k+i|k\right)\right]^2, \tag{6.5}$$

where P is the set of coincidence points where the reference trajectory and the predicted outputs should match. To minimize (6.5) the Levenberg-Marquardt algorithm is used, and the constraints of the system apply both to u and y. The choke opening u, has fully open, u_{max}, and fully closed, u_{min},

as the upper and lower bounds. The annulus BHP y, has reservoir pore pressure, y_{max}, and reservoir collapse pressure, y_{min}, as the upper and lower bounds. The control algorithm is further described and evaluated in [59].

The described model predictive control design is well suited for a multi-variable control design. The cost criterion can easily be revised by adding new measurements such as sensor arrays and control variables such as fluid flow rate and fluid density. Also restrictions of the fluid density and fluid flow rate can be included as limiting factors in the optimization algorithm.

Chapter 7

Paper Presentation

The research context for this project is based on the cooperation between Telemark University College and IRIS Petroleum, and the activities that IRIS Petroleum was engaged in at the start of this research [4, 41, 42, 45, 46]. IRIS Petroleum had developed a dynamic multi-phase well model over a time span of 20 years, and had also implemented various Kalman filters for nonlinear applications and the Levenberg-Marquardt optimization algorithm for solving nonlinear least-squares problems.

Focus has been on UBD operations where one of the primary challenges has been to estimate the reservoir properties based on flow related measurements obtained during the drilling operation. A test rig has been set up at the Telemark University College, and results from this work is presented in Section 5.1.

Several papers from the start of this research discussed reservoir characterization during UBD, such as [26, 36, 37, 40, 44]. All these papers focused on how the reservoir responded to underbalanced drilling, but not taking into account the dynamics of the whole well bore. A transient reservoir model has been implemented and this has been integrated with the established dynamic well model. Analyses have been carried out using an off-line least squares parameter estimation method, utilizing an implementation of the Levenberg-Marquardt optimization algorithm. The work resulted in Paper A.

Further examination of the Levenberg-Marquardt algorithm showed that more information about the reservoir were obtained if the well pressure was subjected to oscillations. The ensemble Kalman filter has also been examined and shown promising results. These examinations resulted in Paper B. At the same time, also other research institutions presented work in this field [6, 27]. At a later stage, Paper B was selected for publication by SPE Journal.

Achieving stable oscillations in the BHP during UBD operations would be

difficult in an actual drilling operation, as the BHP was typically controlled manually by a trained operator, resulting in inaccurate BHP. Some early efforts of providing an automatic choke system had focused on controlling the annulus pressure [70, 81, 84], using direct measurements of the flow rates, pump pressure, choke pressure and if available, also the BHP.

The scope of research in the context of this thesis was now broadened to develop methods that combined both reservoir parameter estimation and control of the BHP. Of special interest was controlling the BHP during a pipe connection procedure. A manual pipe connection procedure was described in [64]. An NMPC algorithm for automating the pipe connection procedure has been developed and presented in Paper C. The method was later extended to also include the whole drilling operation, and this work resulted in Paper D. Several other industrial efforts were made by other companies in developing a choke control system, however, using linear control or semi-automatic methods only [13, 67, 71].

A comparison between linear control and the developed NMPC algorithm has been performed, where a low-order state fluid flow model has been developed [58] for tuning the linear control algorithm. The low-order model development has been inspired by the Petronics project at NTNU [14, 80]. A comparison between linear control and the developed NMPC algorithm resulted in Paper E.

A comparison of the control methods has been further examined for a potential field application [29]. The low-order model has been used for comparison of the performance of various Kalman filters. This work is described in Section 4.3.4, and has been published in a conference paper [60].

As a new, high density data transmission method has been developed [30, 66], a new study has been carried out to evaluate the need for new sensors at new positions during drilling operations. This study is presented in Section 5.2 and Section 5.3, and has been published as a conference paper [57].

A chronological list of the author's publications which has been the outcome of this project is given below:

1. E. H. Vefring, G. Nygaard, K. K. Fjelde, R. J. Lorentzen, G. Nævdal, and A. Merlo. Reservoir characterization during underbalanced drilling: Methodology, accuracy, and necessary data. In *SPE Annual Technical Conference and Exhibition*, number SPE 77530-MS, San Antonio, Texas, USA, September 29 - October 2, 2002.
   (Referred to as Paper A in Part II.)

2. E. H. Vefring, G. Nygaard, R. J. Lorentzen, G. Nævdal, and K. K. Fjelde. Reservoir characterization during UBD: Methodology and active tests. In *IADC/SPE Underbalanced Technology Conference and Exhibition*, number

SPE 81634-MS, Denver, Colorado, USA, March 25-26, 2003.

3. G. H. Nygaard, E. H. Vefring, S. Mylvaganam, R. J. Lorentzen, G. Nævdal, and K. K. Fjelde. Underbalanced drilling: Improving pipe connection procedures using automatic control. In *SPE Annual Technical Conference and Exhibition*, number SPE 90962-MS, Houston, Texas, USA, September 26-29, 2004.
(Referred to as Paper C in Part II.)

4. G. H. Nygaard, E. H. Vefring, K. K. Fjelde, G. Nævdal, R. J. Lorentzen, and S. Mylvaganam. Bottomhole pressure control during pipe connection in gas dominant wells. In *SPE/IADC Underbalanced Technology Conference and Exhibition*, number SPE 91578-MS, The Woodlands, Texas, USA, October 11-12, 2004.
(Referred to as Paper D in Part II.)

5. G. Nygaard and G. Nævdal. Modelling two-phase flow for control design in oil well drilling. In *IEEE Conference on Control Applications*, Toronto, Canada, August 28-31, 2005.

6. G. Nygaard, K. K. Fjelde, G. Nævdal, R. J. Lorentzen, and E. H. Vefring. Evaluation of drillstring and casing instrumentation needed for reservoir characterization during drilling operations. In *SPE/IADC Middle East Drilling Technology Conference and Exhibition*, number SPE 97372-MS, Dubai, U.A.E., September 12-14, 2005.

7. E. H. Vefring, G. Nygaard, R. J. Lorentzen, G. Nævdal, and K. K. Fjelde. Reservoir characterization during underbalanced drilling (UBD): Methodology and active tests. *SPE Journal*, Vol. 11, number SPE 81634-PA:181-192, June 2006.
(Referred to as Paper B in Part II.)

8. G. Nygaard and G. Nævdal. Non-linear model predictive control scheme for stabilizing annulus pressure during oil well drilling. *Journal of Process Control*, 16(7):719-732, 2006.
(Referred to as Paper E in Part II.)

9. G. Nygaard, G. Nævdal and S. Mylvaganam. Evaluating Nonlinear Kalman Filters for Parameter Estimation in Reservoirs During Petroleum Well Drilling. To appear in *IEEE Conference on Control Applications*, München, Germany, October 4-6, 2006.

Paper 1 is included in this thesis as Paper A. Paper 2 is initially published as a conference paper, but appear in revised form as a journal paper, Paper 7, which is included in this thesis as Paper B. Paper 3 is a conference paper which is included in the thesis as Paper C. Paper 4 is a conference paper

which is included in the thesis as Paper D. Paper D is also currently under a peer review process for publication in SPE Journal. Paper 5 is a conference paper and the content of this paper is a part of a journal paper, Paper 8, which is included in the thesis as Paper E. Paper 6 is a conference paper where the content of the paper is based on the results from Section 5.2 and Section 5.3. Paper 9 is a conference paper where the content of the paper is based on the results from Section 4.3.4.

Paper A and Paper B evaluate the possibility of fusing flow related data to estimate reservoir properties. Paper C and D show how the found reservoir properties can be used to assist in controlling the well pressure using an NMPC algorithm. Paper E seizes the essence of the NMPC algorithm and compares it to a simple, conventional control method. The following sections in this chapter summarize the papers, Paper A - Paper E, which are included in Part II of this thesis.

7.1 Paper A: Reservoir Characterization during Underbalanced Drilling: Methodology, Accuracy, and Necessary Data

The focus in Paper A [85] is to estimate reservoir parameters using off-line least squares techniques based on fluid flow related measurements obtained during drilling operations. A transient reservoir model is developed, and coupled with an existing transient well flow model as described in Section 4.2.2. A drilling case is defined and simulated. Synthetic measurements are generated from the simulations by adding an unbiased noise signal to the data. The measurement data are outlet flow rates, pump pressure and BHP, which are usually available while drilling. The liquid injection and gas injection rates are used as input to the model.

A Levenberg-Marquardt algorithm, described in Section 4.3.3, is used to match the measurements with the model, by estimating the model parameters (permeability and reservoir pressure) along the well. Estimating both reservoir permeability and reservoir pressure simultaneously is difficult, and leads to large uncertainties in the reservoir parameter estimates. Under the assumption that the reservoir pressure is known, reliable estimates of the permeability can be obtained. A methodology for uncertainty analysis is also presented and can be used to select necessary measurements for proper reservoir characterization.

7.2 Paper B: Reservoir Characterization during Underbalanced Drilling (UBD): Methodology and Active Tests

In Paper B [87], two different estimation methods are described: history matching using an off-line nonlinear least squares technique utilizing the Levenberg-Marquardt algorithm and data assimilation using the ensemble Kalman filter technique for parameter estimation, described in Section 4.3.4. The focus is to estimate both the pressure and permeability, while performing an excitation of the BHP, trying to get a sufficiently rich signal to be used as basis for the parameter estimation. A mathematical model combining both reservoir dynamics and well fluid dynamics, described in Section 4.2.2, is utilized. The measured data are outlet rates, pump pressure and downhole pressure. The liquid injection and gas injection rates are used as input to the model. The two methodologies are applied to synthetic cases. The simulations show that data assimilation technique gives equivalent results when compared to the post-processing history matching algorithm, but the data assimilation technique is preferred since this analyzes the data in real time.

7.3 Paper C: Underbalanced Drilling: Improving Pipe Connection Procedures Using Automatic Control

In Paper C [62], the NMPC algorithm described in Section 6.2 is introduced to maintain the well pressure within the given limits. The model used for the predictions is the dynamic well-reservoir model from Section 4.2.2, and the optimization step is carried out using the Levenberg-Marquardt algorithm.

The control method has been applied to two different field based cases. The results show that by controlling the choke opening and adjusting the circulation fluid flow rates during a pipe connection, it is possible to reduce the pressure variation in the BHP. By predicting the future behaviour of the well using the dynamic model, an optimal choke setting can be selected. The model is calibrated with the UKF method presented in Section 4.3.4 and using available well measurements.

It was showed that slow ramping of the circulation fluid flow rates before and after pipe connection, while controlling the choke, have most effect in wells with fluids having low compressibility.

7.4 Paper D: Bottomhole Pressure Control During Pipe Connection in Gas-Dominant Wells

Paper D [61] is a further investigation of NMPC for controlling the BHP during UBD operations where the fluid flow is highly gas dominant. The available control actions are the gas injection rate before and after the pipe connection and choke valve settings during the whole UBD operation. Measurement of the pump rates, pump pressures, choke pressure and the BHP are also available to support the control actions.

A field based case with gas injection has been examined using this control methodology. The results show that NMPC can be utilized in developing an integrated pump rate and choke control system for UBD operations.

The future state of the BHP depends to a large extent on the productivity of the reservoir. However, the production rates that can be expected are often unknown in advance. The reservoir model is updated based on measurements of the well using the UKF method. The results indicate that this control methodology might assist in reducing variations in the BHP during UBD.

7.5 Paper E: Non-linear model predictive control scheme for stabilizing annulus pressure during oil well drilling

Paper E [59] compares a manual control procedure with a standard linear controller, presented in Section 6.1, and the NMPC method described in Section 6.2. In the selected test case, the manual control procedure reduces the fluctuations of the BHP, but fails to keep the pressure within the required margins. The linear control method for adjusting the choke valve during UBD operations is able to keep the BHP within the required margins, both during the whole drilling operations and during pipe connection procedures. By using a low-order state model, described in Section 4.2.1, a set of efficient control parameters can be found.

However, if the circulation flow rates are being modified, then the simple low-order state model might not describe the real process with sufficient accuracy. This requires that the low-order model is re-tuned, and that new linear control parameters should be found. The NMPC method based on the detailed model from Section 4.2.2 includes the circulation flow rate in the control calculations, thus it will compensate for such variations.

Chapter 8

Future Directions

Based on the current research results, suggestions for future research directions can be given. The chapter is divided into four topics: modelling, sensors, data fusion and process control. In addition to these specific topics, there are also a need for evaluating the described methods in full scale tests in real-time, and eventually in actual UBD applications.

8.1 Modelling

Both the low-order well model and the detailed well model can be examined further [57, 59]. Since the low-order model is faster computationally than the detailed model, it can be used for calculating predictions further ahead in time than the detailed model. This indicates that the low-order model can be used to predict the low-frequency dynamics of the well, such as long term flow rate variations and fluid density variations.

The detailed model is well suited for predicting the high frequency pressure fluctuations that occur during drilling. Further development of the detailed model would be to include dynamic temperature effects and cuttings transportation inside the annulus section of the well. An improvement of the transient reservoir model would also be of future interest.

8.2 Sensors

Evaluation of more sensors along the drillstring is important to improve the reservoir parameter estimates. Sensors with various physical measurement principles for estimating liquid velocity should be examined. Inclusion of temperature sensors would be of interest for improving the estimation of

reservoir inflow due to the temperature difference between the reservoir fluid and the drilling fluid.

In this thesis, new sensor designs have been suggested to improve the estimation of both drilling fluid properties and reservoir properties. The current analysis indicates that flow data from an annulus flow meter would improve estimation of unknown parameters in the well and reservoir. Further investigation of the feasibility in designing such an annulus flow meter would be of great interest.

Sensor arrays are another sensor design, which can be of interest. The results from the sensor array evaluations indicate that the pressure sensor arrays contain information about the friction pressure loss in the annulus section of the well, and would hence give information abut the fluid velocities. Pressure sensor arrays are currently being developed for production wells, and the data from such sensors could be used also during the drilling phase of the well.

Inclusion of other reservoir data such as the NMR log in addition to the acoustic log could be a basis for further examination.

8.3 Data fusion

Further evaluations of various Kalman filter implementations using real-time data from a full-scale experimental set-up would be interesting. Other estimation techniques such as the H_∞-filtering [75] could be evaluated combined with the low-order dynamic model.

In a typical drilling operation, the data transmission rate is low between the top of the well and the bottomhole sensors. Also during other well operations such as cementing, it is currently not possible to transfer data between the bottomhole of the well and the wellhead. One topic for future research could be in develop and examine a virtual sensor system based on a data fusion algorithm using only data available for sensors placed at the wellhead, such as various flow sensors, pump pressure and choke valve differential pressure. The virtual sensor system could then provide downhole information such as flow rate, pressure and temperature at a higher rate than currently available Measurement-While-Drilling system.

8.4 Process Control

Both linear control and NMPC should be further examined for controlling the BHP in the well. Controlling the choke valve to compensate for pres-

sure fluctuations has shown promising results, and the next step would be to include automatic fluid flow rate control for maintaining sufficient hole cleaning conditions.

The drilling flow rate can only be adjusted over a longer time span than the choke valve, typically at a few minutes time scale. By including automatic handling of the drilling fluid flow, the system can maintain a slowest possible circulation rate to keep a sufficient hole cleaning, and having the choke at the highest opening to avoid choke plugging. Based on calculations using a dynamic model of the complete drilling system, the optimal selection of both the choke setting and the drilling fluid flow rate are found.

A further step ahead will be to include control of the drilling fluid density. This could give the possibility of dynamically adjust the density of the drilling fluid. Change of the fluid density gives a slow response in the BHP, since the new density drilling fluid will have to displace the old fluid before the full pressure effects can be seen.

Controlling the fluid density dynamically raises quite a few issues regarding the process safety with respect to an uncontrolled reservoir influx from the reservoir and into the well. The multivariable control methods developed should be evaluated according to the overall safety regulations issued by the authorities.

Chapter 9

Conclusions

During UBD, data from various sources are available for the operators. As more sensors become available in drilling systems there is a growing need for methods and tools for extracting useful information from the sensor data. MSDF is an overall method for analysing sensor data, where the focus is to extract as much information as possible from the measured data, where one of the goals is to extract information that is not directly measurable.

When evaluating several sensors, the physical properties of the actual process should be examined. A mathematical model which describes the underlying physical dynamics of the fluid flow in addition to the heat transfer, give the possibility of better understanding the data from pressure, flow and temperature measurements coming from the process. By combining dynamic measurements from the process and simulated results from the models, more knowledge about the process can be extracted. This knowledge can then be used for controlling the fluid flow and the pressures in the well.

When performing an UBD operation, reservoir fluids are migrating from the reservoir and into the well. The resulting reservoir influx influences the annulus pressure. To improve the drilling operations, information about the reservoir properties should be made available to the operators. In addition, assistance in maintaining a correct annulus pressure in the well would be helpful for the operators.

The first section in this chapter presents the conclusions of the research regarding reservoir characterization, and the second section presents the conclusions regarding annulus pressure control during drilling.

9.1 Reservoir Characterization

MSDF provides several different algorithms for extracting useful information from available data based on sensors and prior knowledge of the process. Knowledge about fluid flow can be expressed using mathematical models based on known physical relations also called first-principles modelling. These models are often non-linear, and with a high-order state vector. The models are also referred as computational fluid dynamics models and contain detailed information about the fluid flow behaviour. The models describe the dynamics of the well fairly accurate and the calculated flow rates and pressures match quite good to the real measurements. The research results show that a detailed model should be used when evaluating the data from the well, as a low-order are not able to describe the fluid behaviour sufficiently accurate to extract useful information about the reservoir.

An important aspect for reservoir characterization is to select and develop methods for estimating parameters in models that have a high-order state vector. Standard Kalman filter methods such as the extended Kalman filter for non-linear systems are computational intensive, since the method requires a linearization of the model. Only sensor data usually measured during an UBD operation is used for calibrating the model. The research results show that the data should be evaluated in real-time and that post-processing analysis is not able to extract more information from the data when compared to real-time analysis.

Both single-phase fluid flow wells and two-phase fluid flow wells have been considered. The few examples presented in the current work indicate that it is difficult to estimate both permeability and reservoir pressure from a reservoir with several zones. However, if the reservoir pressure is known, reliable estimates of the permeability are obtained. A methodology for uncertainty analysis has also been presented and can be used to evaluate necessary measurements for proper reservoir characterization. The research results show that when evaluating the reservoir properties when using a multi-phase drilling fluid, the multi-phase fluid model needs to be calibrated using available fluid flow data.

Some of the obtained results in Paper B did not show significant differences between the parameter estimation results obtained with least squares estimation and with ensemble Kalman filter. However, the advantage of the ensemble Kalman filter is that the parameter estimates can be obtained during drilling. The unscented Kalman filter has also been evaluated for estimation of reservoir parameters and fluid parameters. This filter has shown to give good parameter estimates, and has shown to be less computational intensive than the ensemble Kalman filter when used for model parameter es-

timation. The research results in this thesis show that the unscented Kalman filter parameter estimation is a good candidate for further analysis when using the model for pressure control, as the calculation resources required are less than for the ensemble Kalman filter.

9.2 Pressure Control during Drilling

Automatic control of the well pressures during drilling reduces the transient fluctuations during specific operations such as pipe connections. Multivariable control is a challenging task, but it is crucial to combine the control of fluid flow rate and choke valve opening since both influence the BHP. The research results show that only using choke valve for manipulating the pressure gives sufficient results, but that fluid flow rate control would increase the ability of maintaining the correct pressure during the whole drilling operation.

Two different control algorithms have been evaluated, a linear control algorithm and an NMPC algorithm. The results show that both these algorithms are able to reduce the pressure fluctuations during pipe connections when comparing them with manual procedures. The NMPC algorithm is more computational intensive, but the algorithm is easier to expand to handle multiple control variables and constraints.

The research results show that the model predictive control algorithm is a good candidate for performing pressure control during drilling, when used together with a detailed model. The low-order model could be used for long time predictions when including fluid density control.

Bibliography

[1] BakerHughes. Multiple propagation resistivity tool. Internet url, http://www.bakerhughes.com, February 2006.

[2] J. G. Balchen, M. Fjeld, and O. A. Solheim. *Reguleringsteknikk, Bind 3*. Tapir, Trondheim, Norway, 1978.

[3] J. G. Balchen and K. I. Mumme. *Process Control. Structures and applications*. VanNostrand Reinhold, New York, USA, 1988.

[4] A. M. Berg, G. Nævdal, E. H. Vefring, S. I. Aanonsen, Y. Soni, and M. Kaja. Downhole monitoring systems for estimating inflow profiles. In *Proceedings for the SPE/DOE Thirteenth Symposium on Improved Oil Recovery*, number SPE 75260, Tulsa, Oklahoma, U.S.A., April 13–17, 2002.

[5] L. E. Berg. *Programutvikling for tekniske anvendelser*. Fagbokforlaget, Bergen, Norway, 1998.

[6] D. Biswas, P.V. Suryanarayana, P.J. Frink, and S. Rahman. An improved model to predict reservoir characteristics during underbalanced drilling. In *SPE Annual Technical Conference and Exhibition*, number SPE 84176, Denver, Colorado, USA, October 5–8, 2003.

[7] R.R. Brooks and S.S. Iyengar. *Multi-sensor fusion: fundamentals and applications with software*. Prentice Hall PTR, Upper Saddle River, N.J., 1998.

[8] R. G. Brown and P. Y. C. Hwang. *Introduction to random signals and applied Kalman filtering*. John Wiley & Sons, New York, USA, 1997.

[9] N. Chaiyaratana. Overview of genetic algorithms. Unpublished, 2002.

[10] ClampOn. Clampon DSP Particle Monitor. Internet url, http://www.clampon.no, February 2006.

[11] L. P. Dake. *Fundamentals of reservoir engineering*, volume 8 of *Developments in petroleum science*. Elsevier, Amsterdam, The Netherlands, 1978.

[12] L. J. Durlofsky and K. Aziz. Advanced techniques for reservoir simulation and modeling of nonconventional wells. Technical Report DE-AC26-99BC15213, Stanford University, Stanford, California, August 2004.

[13] J. Eck-Olsen, P. J. Pettersen, A. Rønneberg, K. S. Bjørkevoll, and R. Rommetveit. Managing pressures during underbalanced cementing by choking the return flow; innovative design and operational modeling as well as operational lessons. In *Proceedings for the SPE/IADC Drilling Conference*, number SPE/IADC 92568, Amsterdam, The Netherlands, February 23–25, 2005.

[14] G. O. Eikrem, L. Imsland, and B. A. Foss. Stabilization of gas-lifted wells based on state estimation. In *IFAC International Symposium on Advanced Control of Chemical Processes*, Hong Kong, China, January 11–14, 2004.

[15] G. Evensen. Sequential data assimilation with a nonlinear quasi-geostrophic model using Monte Carlo methods to forecast error statistics. *Journal of Geophysical Research*, 99(C5):10143–10162, 1994.

[16] G. Evensen. The ensemble Kalman filter: theoretical formulation and practical implementation. *Ocean Dynamics*, 53:343–367, 2003.

[17] T. Fallet, B. Raad, and M. H. Jensen. A high temperature electronic system for monitoring and control of intelligent oil wells, 2000.

[18] E. Framnes. *Boreteknologi*. Vett&Viten, Oslo, Norway, 1993.

[19] P. E. Gill. *Practical Optimization*. Academic Press, San Diego, USA, 1981.

[20] M. Golan and C.H. Whitson. *Well performance*. Tapir, Trondheim, Norway, second edition, 1996.

[21] M. T. Hagan, H. B. Demuth, and M. Beale. *Neural Network Design*. PWS Publishing Company, Boston, Massachusetts, 1995.

[22] D. Hanselman and B. Littlefield. *Mastering MATLAB 6*. PrenticeHall, New Jersey, USA, 2001.

[23] F. Haugen. *Regulering av dynamiske systemer*. Tapir, Trondheim, Norway, 1994.

[24] B. T. Hjertaker, S. A. Tjugum, E. A. Hammer, and G. A. Johansen. Multimodality tomography for multiphase hydrocarbon flow measurements. *IEEE Sensors Journal*, 5(2):153–160, April 2005.

[25] M. B. Holstad, G. A. Johansen, P. Jackson, and K. S. Eidsnes. Scattered gamma radiation utilized for level measurements in gravitational separators. *IEEE Sensors Journal*, 5(2):175–182, April 2005.

[26] J. L. Hunt and S. Rester. Reservoir characterization during underbalanced drilling: A new model. In *Proceedings for the SPE/CERI Gas Technology Symposium*, number SPE 59743, Calgary, Alberta, Canada, April 3–5, 2000.

[27] J. L. Hunt and S. Rester. Multilayer reservoir model enables more complete reservoir characterization during underbalanced drilling. In *IADC/SPE Underbalanced Technology Conference and Exhibition*, number SPE 81638, Denver, Colorado ,USA, March 25–26, 2003.

[28] M. Ishii. *Thermo-Fluid Dynamic Theory of Two-Phase Flow*. Eyrolles, 1975.

[29] F. Iversen, J. E. Gravdal, G. Nygaard, H. Gjeraldstveit, E. W. Dvergsnes, and L. A. Carlsen. Kvitebjørn MPD assessment study. Technical Report RF-2005/267, RF - Rogaland Research, Bergen, Norway, 2005.

[30] M. J. Jellison, R. Urbanowski, H. Sporker, and M. E. Reeves. Intelligent drill pipe improves drilling efficiency, enhances well safety and provides added value. In *IADC World Drilling Conference*, Dubrovnik, Croatia, July 1–2, 2004.

[31] J. W. Jenner, H. L. Elkins, F. Springett, P. G. Lurie, and J. S. Wellings. The continuous circulations system: An advance in constant pressure drilling. In *SPE Annual Technical Conference and Exhibition*, number SPE 90702, Houston, Texas, USA, September 26–29, 2004.

[32] S. Julier and J.K. Uhlmann. Data fusion in nonlinear systems. In D. L. Hall and J. Llinas, editors, *Handbook of Multisensor Data Fusion*, chapter 13. CRC Press, Boca Raton, Florida, 2001.

[33] S. J. Julier and J. K. Uhlmann. Unscented filtering and nonlinear estimation. *Proceedings of the IEEE*, 92(3):401–422, March 2004.

[34] S. J. Julier, and J. K. Uhlmann. Reduced Sigma Point Filters for the Propagation of Means and Covariances through Nonlinear Transformations. In *Proceedings of the IEEE American Control Conference*, pages 887–892, Anchorage AK, USA, 8–10 May 2002.

[35] S. J. Julier, and J. K. Uhlmann. The Scaled Unscented Transformation. In *Proceedings of the IEEE American Control Conference*, pages 4555–4559, Anchorage AK, USA, 8–10 May 2002.

[36] C. B. Kardolus and C. P. J. W. Kruijsdijk. Formation testing while underbalanced drilling. In *Proceedings for the SPE Annual Technical Conference and Exhibition*, number SPE 38754, San Antonio, Texas, October 5–8, 1997.

[37] W. Kneissl. Reservoir characterization whilst underbalanced drilling. In *Proceedings for the SPE/IADC Drilling Conference*, number SPE/IADC 67690, Amsterdam, The Netherlands, February 27–1, 2001.

[38] T.K. Kragas, F.X.Bostick III, C. Mayeu, D. L. Gysling, and A. M. van der Spek. Downhole fiber-optic flowmeter: Design operating principle, testing, and field installations. *SPE Production and Facilities*, (SPE 87086):257–268, November 2003.

[39] T. Kristensen. *Nevrale nettverk, fuzzy logikk og genetiske algoritmer.* Cappelen Akademisk Forlag, Oslo, Norway, 1997.

[40] C. P. J. W. Kruijsdijk and R. J. W. Cox. Testing while underbalanced drilling: Horizontal well permeability profiles. In *SPE European Formation Damage Conference*, number SPE 54717, The Hague, The Netherlands, May 31–1, 1999.

[41] A. C. V. M. Lage. *Two-phase Flow Models and Experiments for Low-Head and Underbalanced Drilling.* PhD thesis, Stavanger University College, Stavanger, Norway, September 2000.

[42] A. C. V. M. Lage, J. Frøyen, O. Sævareid, and K. K. Fjelde. Underbalanced drilling dynamics: Two-phase flow modelling, experiments and numerical solutions techniques. In *Proceedings of The Rio Oil & Gas Conference*, Rio de Janeiro, Brazil, October 16–19, 2000.

[43] A.C.V.M. Lage, E. Nakagawa, P. H. de Andrade Jr., P. R. C. Silva, and V. Silva Jr. Full scale aerated fluids experiments in Taquipe BA Phase II. Technical Report RF-98/245, RF - Rogaland Research, Bergen, Norway, 1998.

[44] L. Larsen and F. Nilsen. Inflow predictions and testing while underbalanced drilling. In *Proceedings for the SPE Annual Technical Conference and Exhibition*, number SPE 56684, Houston, Texas, October 3–6, 1999.

[45] R. J. Lorentzen, K. K. Fjelde, F. Frøyen, A. C. V. M. Lage, G. Nævdal, and E. H. Vefring. Underbalanced and low-head drilling operations: Real time interpretation of measured data and operational support. In *SPE Annual Technical Conference and Exhibition*, number SPE 71384, New Orleans, Louisiana, USA, September 30–3, 2001.

[46] R. J. Lorentzen, G. Nævdal K. K. Fjelde F. Frøyen, A. C. V. M. Lage, and E. H. Vefring. Underbalanced drilling: Real time data interpretation and decision support. In *Proceedings for the SPE/IADC Drilling Conference*, number SPE/IADC 67693, Amsterdam, The Netherlands, February 27–1, 2001.

[47] D. G. Luenberger. *Linear and Nonlinear Programming*. Addison-Wesley Publishing, Reading, Massachusetts, 1984.

[48] W. C. Lyons, B. Guo, and F. A. Seidel. *Air and Gas Drilling Manual*. McGraw-Hill, New York, NY, 2001.

[49] W. C. Lyons and G.J. Plisga, editors. *Standard handbook of petroleum and natural gas engineering*. Elsevier, Amsterdam, The Netherlands, 2005.

[50] J. M. Maciejowski. *Predictive Control with Constraints*. PrenticeHall, Harlow, England, 2002.

[51] B. Massey and J. Ward-Smith. *Mechanics of fluids*. Taylor & Francis, London, UK, eigth edition, 2006.

[52] A. E. Mengen. Application of different optimization techniques to parameter estimation from interference well test data. M.Sc. thesis, Istanbul Technical University, Istanbul, Turkey, January 2004.

[53] J. J. Moré. The Levenberg-Marquardt algorithm: Implementation and theory. In G. A. Watson, editor, *Numerical Analysis*, volume 630 of *Lecture Notes in Mathematics*. Springer Verlag, Berlin, Germany, 1977.

[54] S. Mylvaganam. Some applications of acoustic emission in particle science and technology. *Particle Science and Technology*, 21(3), 2003.

[55] G. Nævdal, E. H. Vefring, A. M. Berg, T. Mannseth, and J. E. Nordtvedt. A new methodology for the optimization of the placement of downhole production-monitoring sensors. *SPE Journal*, pages 108–116, March 2001.

[56] NationalInstruments. Data aquisition. Internet url, http://www.ni.com, August 2006.

[57] G. Nygaard, K. K. Fjelde, G. Nævdal, R. J. Lorentzen, and E. H. Vefring. Evaluation of drillstring and casing instrumentation needed for reservoir characterization during drilling operations. In *SPE/IADC Middle East Drilling Technology Conference and Exhibition*, number SPE 97372, Dubai, U.A.E., September 12–14, 2005.

[58] G. Nygaard and G. Nævdal. Modelling two-phase flow for control design in oil well drilling. In *IEEE Conference on Control Applications*, Toronto, Canada, August 28–31, 2005.

[59] G. Nygaard and G. Nævdal. Non-linear model predictive control scheme for stabilizing annulus pressure during oil well drilling. *Journal of Process Control*, 16(7):719–732, 2006.

[60] G. Nygaard, G. Nævdal, and S. Mylvaganam. Evaluating nonlinear Kalman filters for parameter estimation in reservoirs during petroleum well drilling. In *IEEE Conference on Control Applications*, München, Germany, October 4–6, 2006.

[61] G. H. Nygaard, E. H. Vefring, K. K. Fjelde, G. Nævdal, R. J. Lorentzen, and S. Mylvaganam. Bottomhole pressure control during pipe connection in gas dominant wells. In *SPE/IADC Underbalanced Technology Conference and Exhibition*, number SPE 91578, The Woodlands, Texas, USA, October 11–12, 2004.

[62] G. H. Nygaard, E. H. Vefring, S. Mylvaganam, R. J. Lorentzen, G. Nævdal, and K. K. Fjelde. Underbalanced drilling: Improving pipe connection procedures using automatic control. In *SPE Annual Technical Conference and Exhibition*, number SPE 90962, Houston, Texas, USA, September 26–29, 2004.

[63] M. Onur, P. S. Hegeman, and F. J. Kuchuk. Pressure-transient analysis of dual packer-probe wireline formation testers in slanted wells. In

SPE Annual Technical Conference and Exhibition, number SPE 90250, Houston, Texas, USA, September 26–29, 2004.

[64] C. Perez-Tellez, J. R. Smith, and J. K. Edwards. Improved bottomhole pressure control for underbalanced drilling operations. In *Proceedings for the IADC/SPE Drilling Conference*, number SPE 87225, Dallas, Texas, USA, March 2–4, 2004.

[65] S. J. Pirson. *Geologic Well Log Analysis*. Gulf Publishing Company, Houston, Texas, 1983.

[66] M. E. Reeves, M. L. Payna, A. G. Ismayilov, and M. J. Jellison. Intelligent drill string field trials demonstrate technology functionality. In *SPE/IADC Drilling Conference*, number SPE 92477, Amsterdam, The Netherlands, February 23–25, 2005.

[67] D. Reitsma and E. van Riet. Utilizing an automated pressure control system for managed pressure drilling in mature offshore oilfields. In *Proceedings for SPE Offshore Europe Conference*, number SPE 96646, Aberdeen, United Kingdom, September 6–9, 2005.

[68] M. Rider. *The Geological Interpretation Of Well Logs*. Whittles Publishing, Sutherland, Scotland, 1996.

[69] Roxar. Multiphase meter. Internet url, http://www.roxar.com, February 2006.

[70] H. Santos, C. Leuchtenberg, and S. Shayegi. Micro-flux control: The next generation in drilling process. In *Proceedings for the SPE Latin American and Caribbean Petroleum Engineering Conference*, number SPE 81183, Port-of-Spain, Trinidad and Tobago, April 27–30, 2003.

[71] H. Santos, P. Reid, J. Jones, and J. McCaskill. Developing the micro-flux control method part 1: System development, field test preparation, and results. In *Proceedings for the SPE/IADC Middle East Drilling Technology Conference and Exhibition*, number SPE/IADC 97025, Dubai, United Arab Emirates, September 12–14, 2005.

[72] J. J. Schubert, H. C. Juvkam-Wold, and J. Choe. Well control procedures for dual gradient as compared to conventional riser drilling. In *Proceedings for the SPE/IADC Drilling Conference*, number SPE/IADC 79880, Amsterdam, The Netherlands, February 19–21, 2003.

[73] G. A. F. Seber and C. J. Wild. *Nonlinear Regression*. Wiley, New York, USA, 1989.

[74] R. C. Selley. *Elements of Petroleum Geology*. Academic Press, London, England, second edition, 1998.

[75] D. Simon. From here to infinity. *Embedded Systems Programming*, pages 20–32, October 2001.

[76] D. Simon. Kalman filtering. *Embedded Systems Programming*, pages 72–79, June 2001.

[77] S. Skogestad and I. Postlethwaite. *Multivariable feedback control : analysis and design*. Wiley, Chichester, 1996.

[78] A. N. Steinberg and C. L. Bowman. Revisions to the JDL data fusion model. In D. L. Hall and J. Llinas, editors, *Handbook of Multisensor Data Fusion*, chapter 2. CRC Press, Boca Raton, Florida, 2001.

[79] G. Stephanopoulos. *Chemical Process Control*. PrenticeHall Int., New Jersey, 1984.

[80] E. Storkaas, S. Skogestad, and J. M. Godhavn. A low-dimensional dynamic model of severe slugging for control design and analysis. In *Multiphase'03*, San Remo, Italy, June 11–13, 2003.

[81] R. Suter. Flow and pressure control system. UBD-10 Choke. In *Proceedings of the IADC Underbalanced Drilling Conference and Exhibition*, The Hague, The Netherlands, October 27–28, 1999.

[82] Y. Taitel and D. Barnea. Counter current gas-liquid vertical flow, model for flow pattern and pressure drop. *International Journal of Multiphase Flow*, 9:637–647, 1983.

[83] R. van der Merve and E. A. Wan. The square-root unscented Kalman filter for state and parameter estimation. In *Proceedings of the International Conference on Acoustics, Speech and Signal Processing*, Salt Lake City, USA, May 2001. ICASSP.

[84] E. van Riet, D. Reitsma, and B. Vandecraen. Development and testing of a fully automated system to accurately control downhole pressure during drilling operations. In *Proceedings for the SPE/IADC Middle East Drilling Technology Conference and Exhibition*, number SPE/IADC 85310, Abu Dhabi, United Arab Emirates, October 20–22, 2003.

[85] E. H. Vefring, G. Nygaard, K. K. Fjelde, R. J. Lorentzen, G. Nævdal, and A. Merlo. Reservoir characterization during underbalanced drilling: Methodology, accuracy, and necessary data. In *SPE Annual Technical Conference and Exhibition*, number SPE 77530, San Antonio, Texas, USA, September 29–2, 2002.

[86] E. H. Vefring, G. Nygaard, R. J. Lorentzen, G. Nævdal, and K. K. Fjelde. Reservoir characterization during ubd: Methodology and active tests. In *IADC/SPE Underbalanced Technology Conference and Exhibition*, number SPE 81634-MS, Denver, Colorado ,USA, March 25–26, 2003.

[87] E. H. Vefring, G. Nygaard, R. J. Lorentzen, G. Nævdal, and K. K. Fjelde. Reservoir characterization during underbalanced drilling (ubd): Methodology and active tests. *SPE Journal*, 11(SPE 81634-PA):181–192, June 2006.

[88] VortexVentures. Multidensity speed mixer. Internet url, http://www.vortexventures.com, August 2006.

[89] E. A. Wan and R. van der Merve. The unscented Kalman filter. In S. Haykin, editor, *Kalman Filtering and Neural Networks*, chapter 7. Wiley, New York, 2001.

[90] Weatherford. Optical fiber technology. Internet url, http://www.weatherford.com, February 2006.

[91] F. M. White. *Fluid Mechanics*. McGraw-Hill Int., Boston, USA, fourth edition, 1999.

[92] J. J. Xaio, O. Shoham, and J. P. Brill. A comprehensive mechanistic model for two-phase flow in pipelines. In *SPE Annual Technical Conference and Exhibition*, number SPE 20631, New Orleans, Lousiana, USA, September 23–26, 1990.